

Consequences of environmental heterogeneity for the photosynthetic light environment of a tropical forest

Geoffrey G. Parker^a, David R. Fitzjarrald^{b,*}, Irene Cibelle Gonçalves Sampaio^c

^a Smithsonian Environmental Research Center, Edgewater, MD, USA

^b Atmospheric Sciences Research Center, University at Albany, SUNY, Albany, NY, USA

^c Universidade Federal do Oeste do Pará, Santarém, Pará, Brazil

ARTICLE INFO

Keywords:

Canopy light environment
Diffuse radiation
Forest structure
Northeastern amazon
PPFD
Reflectivity

ABSTRACT

We studied the interplay of atmospheric and canopy structure factors driving the canopy light environment (Photosynthetic Photon Flux Density, PPFD) in primary moist tropical forest in the Tapajós National Forest, Brazil. We quantified the temporal and spatial length scales that characterize intact rain forest inhomogeneities, asking: Are seasonal changes in the canopy radiation balance evident at these scales? We sought to describe the components of intensity, duration and spatial variation of within-canopy PPFD in light of these inhomogeneities. Do fluctuating atmospheric conditions, especially the presence of clouds and precipitation, affect the radiative inputs at both the canopy top and the forest floor?

We examined the characteristic scales of heterogeneity in the vertical and the horizontal using a two-part approach. For radiation we combined long-term continuous high-frequency measurements of down- and up-welling short-wave and visible wavebands above the canopy with similarly frequent observations from a dense sensor network at forest floor. Vertical variations in canopy structure, obtained with a ground-based LIDAR, similarly combined intensive observations at the sensor network with occasional large-scale transects along the forest floor. Close similarities in both radiation and canopy structure at both scales support the representativeness of local observations of the wider area.

A composite broadband measure similar to the Normalized Difference Vegetation Index (denoted cbNDVI) was constructed from above-canopy observations to compare with reports of remotely sensed canopy reflectivity at this site. We estimated the canopy Leaf Area Index (LAI) by combining observations of the variation in understory transmittance by solar elevation with a commonly-used algorithm. We obtained the conventional whole-canopy extinction coefficient, by applying the Beer-Lambert law.

Over the course of a year this forest receives $11,795 \text{ mol m}^{-2}$, only 62% of potential clear-day PPFD – atmospheric transmissivity is reduced by clouds, precipitation, smoke and haze. Very little PAR ($\approx 2\%$) is reflected from the canopy and only 5.7% penetrates to 1 m above the forest floor - overall 92% of PAR is absorbed by the canopy. All radiation balance components closely tracked the dynamics of incoming light, showing little seasonal variation.

Understory light observations across the 7.5–28.5 m spanning the understory array sensors showed essentially constant correlation between sensor pairs over time. There was a high degree of local persistence in the understory spatial pattern that varied slowly and directionally with the changing geometry of the sun and canopy structure. Over larger distances (to 1000 m), the patterns of spatial autocorrelation of understory PPFD and outer canopy structure were remarkably similar in shape, both declining rapidly to a more-or-less constant level around 15–20 m, a scale consistent with the dimensions of outer canopy crowns.

The vertical pattern of transmission and absorption was estimated by combining understory transmittance with the distribution of canopy surface area obtained from the ground-based LIDAR system. It showed the maximum absorption relatively low in the canopy (8–19 m above ground). Although rather tall (canopy height is at 41.5 m), the extremely elaborate outer surface of the forest suggests the layers highest above ground are of little consequence to the PAR absorption budget.

The cbNDVI measure exhibited seasonal variation consistent with other reports (somewhat higher in the wet season) but in contrast to a recent argument that the forest ‘greens up’ during the early dry season. However, except for the variations caused by the angle and intensity of incoming light modulated by atmospheric effects,

* Corresponding author.

E-mail address: dfitzjarrald@albany.edu (D.R. Fitzjarrald).

there was little seasonality in the forest light environment at km67, including: canopy reflectances in several wavebands, all PPFD radiation budget components, the estimated LAI and mid-day PAR extinction coefficient and the length scales of understory PPFD. Canopy transmission was somewhat greater (6.4%) under diffuse skies compared to the least diffuse conditions (6.0%), and slightly more PPFD was absorbed under diffuse (92.7%) versus the least diffuse conditions (92.3%), but was not a significant contribution to the budget.

The large diurnal variations in the extinction coefficient seriously affects its utility as a descriptor of canopy radiative properties. We propose an alternative approach for transmitted light: the canopy behaves as: 1.) a constant fraction filter under diffuse conditions, combined with 2.) a variable filter depending on solar elevation for sunfleck conditions. These regimes may be described with simple parameters each having mechanistic relations to canopy structure. In summary, we demonstrate that obtaining the radiation signal at forest floor at high data rate for long periods exploits seasonal sun angle changes to probe canopy structure. Combined with occasional long transect information, temporal and vertical sampling spatially allow improved definition of characteristic scales to describe both the understory light environment and canopy structure.

1. Introduction

Observations of forest canopy light environment, specifically the various fluxes of Photosynthetically Active Radiation (PAR, 400–700 nm), are central to understanding a variety of structural and functional aspects of forests. First, it is important for estimating the availability of energy for production. Many microclimate features of physiological interest (e.g., humidity and heat) are related to radiation. Canopy radiative properties are also important for large-scale estimates of production and ecosystem status. Next, the details of photon-vegetation interactions are well studied and supported by many well-developed theories. Finally, we note that light is straightforward to measure and has a substantial relevant literature.

Nearly all reports of forest light have focused on selected locations (at the forest floor or within a portion of the canopy), for varying periods, with various levels of replication, sampling frequency, and sensor types. Researchers have pursued two related goals—describing the light environment and inferring vegetation structure—using the same techniques, sometimes combining objectives. Consequently, making direct comparisons among studies is challenging. Only a few studies of canopy light environments have taken explicit account of the external environment (Black et al., 1991; Price and Black, 1990; Moore et al., 1996; Freedman et al., 2001; Vourlitis et al., 2004) and none have specifically considered regional climatic influences, such as cloud presence. Direct observations of vertical patterns of canopy PPFD are fewer still (Yoda, 1978; Marques Filho and Dallarosa, 2001; Wirth et al., 2001; Anhuf and Rollenbeck, 2001; Parker et al., 2005). Except for some crane-based observations (Anhuf and Rollenbeck, 2001; Yoshimura and Yamashita, 2012), these studies were hampered by limited spatial representation, owing to the difficulties of sampling in three dimensions. Recently there have been attempts to estimate within-canopy light environments using remote sensing observation of canopy structure, most commonly with airborne LIDAR (Parker et al., 2001, 2004b; Todd et al., 2003; Kotchenova et al., 2004; Thomas et al., 2006; Lee et al., 2009; Yoshimura and Yamashita, 2012; Stark et al., 2012; Tang et al., 2012).

Since Ashton (1958), the majority of studies of PPFD in tropical forests report measurements made in the understory (e.g., Grubb and Whitmore, 1967; Brinkmann, 1971; Bjorkman and Ludlow, 1972; Chazdon and Fetterer, 1984; Lee, 1989; Torquebiau, 1988; Janúario et al., 1992; Clark et al., 1996; Wandelli and Marques Filho, 1999; Marques Filho and Dallarosa, 2000; Vierling and Wessman, 2000; Montgomery and Chazdon, 2001; Cournac et al., 2002; Marques Filho et al., 2005). Many recent studies of understory light were motivated by providing LAI estimates (de Wasseige et al., 2003; Domingues et al., 2005; Marques Filho et al., 2005; Rivard and Quesada, 2005; Emmons et al., 2006; Doughty et al., 2010). In these reports, fractional illumination ranged between 0.02–0.07 at 0.3–1.0 m above the forest floor, in concert with the review of Baldocchi and Collineau (1994).

Measurements of reflected radiation from the canopy top, the basis

for many remotely sensed estimates of leaf area, ‘greenness’ and other properties, are severely restricted by the need for cloud-free scenes, especially uncommon in the moist tropics in the daytime. Clouds are an essential feature of the Amazon Basin environment (Asner, 2001). Basin-wide greenness estimates have been based on limited areal coverage (Saleska et al., 2003; Samanta et al., 2012) and are often infrequent ‘snapshots’, often at a single time of day. These limitations have fed an ongoing debate revolving about seasonal changes in vegetation indices, as researchers attribute seasonal variations to changes in leaf properties and leaf area (Saleska et al., 2007; Samanta et al., 2010). Morton et al. (2014) argued that much of the entire seasonal variation was an artifact of sensor sensitivity to sun- and view-angle geometry. Li and Min (2013) used a cloud-insensitive microwave vegetation index to study the seasonal leaf area variation, and found no anomalous dry-season green-up.

We measured components of forest PPFD at a site well studied for related processes. We aimed to quantify the length scales that characterize intact rain forest inhomogeneities. Moreover, we wanted to discover whether comparable scales of canopy variation can be inferred from both a small sensor network operating continuously and from occasional sampling on long transects with LIDAR-derived canopy structure. We wanted to know if seasonal changes in the canopy radiation balance are evident at these scales. We sought to describe the components of intensity, duration and spatial variation of ground-level PPFD. Finally, we wanted to discover if fluctuating atmospheric conditions, especially the presence of clouds and precipitation, affect the radiative inputs at both the canopy top and the forest floor.

2. Methods

We combined continuous high-frequency measurements of solar radiation above and below the canopy in primary moist tropical forest and estimated cloud cover fraction using a laser ceilometer, all recorded simultaneously. We combined these with observations of canopy structure made with a portable LIDAR. From these data, we describe the canopy reflectance and understory transmittance of Photosynthetic Photon Flux Density (PPFD), the balance of direct and diffuse fractions, and the whole canopy budget of PPFD. We examine the dependence of transmittance and the probability and duration of sun-flecks on solar elevation angle, season, and sky conditions. From co-located measurements of PPFD and LIDAR structure along three 1000 m transects, we explore the relationship between transmission and overhead vegetative cover, surface area density, and local canopy height. From the height distribution of canopy surface area density, we estimate the mean vertical pattern of within-canopy transmittance and absorbance. We demonstrate how seasonal differences in the atmospheric environment alter the daily course of incoming PPFD. Finally, we propose an approach for reporting canopy transmittance that permits comparisons among studies.

2.1. Site description

We conducted this study in the Tapajós National Forest (TNF) in Pará state, Brazil ($2^{\circ}51' S$, $54^{\circ}58' W$) at a site accessed approximately 67 km south of Santarém along the BR 163 highway (hereafter km67; Fig. 1). This site was a focus of ecological and boundary layer studies [project CD-03] under the Large-Scale Atmosphere-Biosphere Experiment in Amazonia (LBA) (Davidson and Artaxo, 2004; Keller et al., 2004). Mean annual temperature and precipitation for the site are $25.8 \pm 1.5^{\circ}C$ and 1800 ± 225 mm (Fitzjarrald et al., 2008).

Based on inspection of the seasonality of precipitation from long-term records from Belterra, 60 km north of the km67 site, we defined the reliably dry (July 13 through November 17, days 195–319, 9.5% of annual precipitation) and wet (January 18 through May 14, days 15–135, 60.1%) seasons, resulting in seasons with roughly the same length. The intervening transition seasons varied in precipitation totals from year to year. The nearly equatorial location assured that solar elevation rose to 90° , except during the transition and rainy seasons (Fig. 2).

The surrounding vegetation is “closed tropical rainforest with emergents on flat, upland terrain...”, “...characterized by emergent species such as *Bertholletia excelsa*, *Couratari* spp., *Dinizia excelsa*, *Hymenaea courbaril*, *Manilkara huberi*, *Parkia* spp., *Pithecellobium* spp. and *Tabebuia serratifolia*” (Parrotta et al., 1995). The maximum canopy height is 42 m with total (above- and below-ground) biomass (at km67: de Castilho et al., 2006; near km 83: Keller et al., 2001) of ≈ 372 Mg ha^{-1} , aboveground biometrical observations indicating small but variable annual growth (0.8 ± 2 Mg C $ha^{-1} yr^{-1}$; Miller et al., 2004), a Leaf Area Index (LAI) of 5.07 (Malhado et al., 2009; values from other sites are reported by McWilliam et al., 1993; Williams et al., 1998;

Domingues et al., 2005; Mahli et al., 2009; Brando et al., 2010), well-known recent disturbance history (Chambers et al., 2001; Keller et al., 2001; Asner et al., 2004; Miller et al., 2004) and extensive turbulence flux measures of Net Ecosystem Exchange of CO₂ (Saleska et al., 2003; Viera et al., 2004; Hutyra et al., 2005; Pyle et al., 2008).

2.2. Incident radiation measurements

Our four-component net radiometer (CNR1; Kipp and Zonen, Delft, The Netherlands), mounted on the tower at 64.2 m, well above the canopy outer canopy surface, yielded observations of total energy from up- and down-facing sensors in both short- (pyranometer, S) and long-wave (pyrgeometer, L) bands. The pyranometer fluxes are termed S_{up} and S_{dw} respectively. Up- and down-facing PAR quantum sensors (LI190; LI – COR, Lincoln, NB) were co-located with the net radiometer. The PAR fluxes are termed PPFD_{up} and PPFD_{dw}, respectively. The sensors were new and recently calibrated. All external radiation observations were recorded every 5 s. Similar observations of solar radiation were taken at another nearby forested ('km83,' 18 km S). At the pasture site ('km77,' 20 km SSE; Fig. 1), our group deployed identical radiation instruments with the same recording protocols. This was the nearest site of a regional meteorological network in operation during the study (Fitzjarrald et al., 2008).

From April 2001 through June 2003 a Vaisala CT-25 K Ceilometer (Helsinki, Finland) provided 15-s measurements of cloud base (three levels up to 7500 m), echo intensity and a 15-s backscatter profile with 30 m resolution. Cloud cover fraction was obtained by the fraction of time the ceilometer reported cloud base (Czikowsky and Fitzjarrald, 2009). Rainfall was measured with a tipping bucket gage (TE525; Texas Electronics, Dallas TX) at 43 m on the tower, recording precipitation

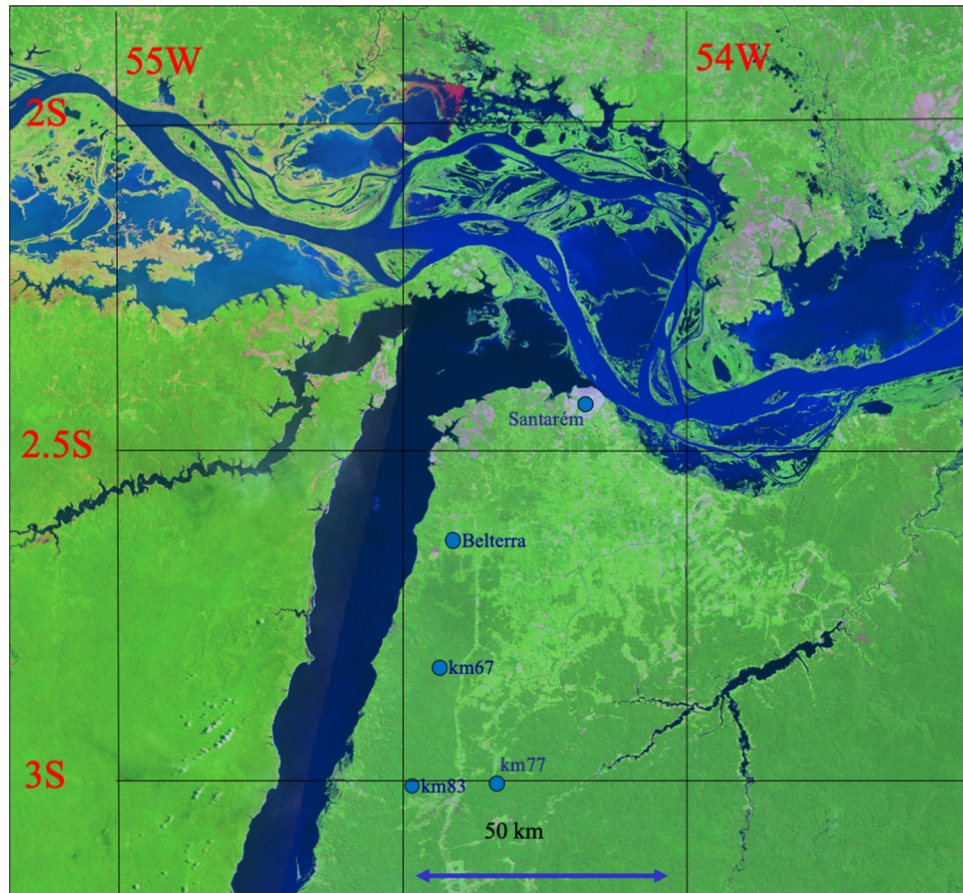


Fig. 1. Location of the km67 (intact forest), km83 (partially logged) and km77 (pasture) sites, the Tapajós National Forest, the city of Santarém and the nearby Tapajós (to the West) and Amazon (to the North) Rivers.

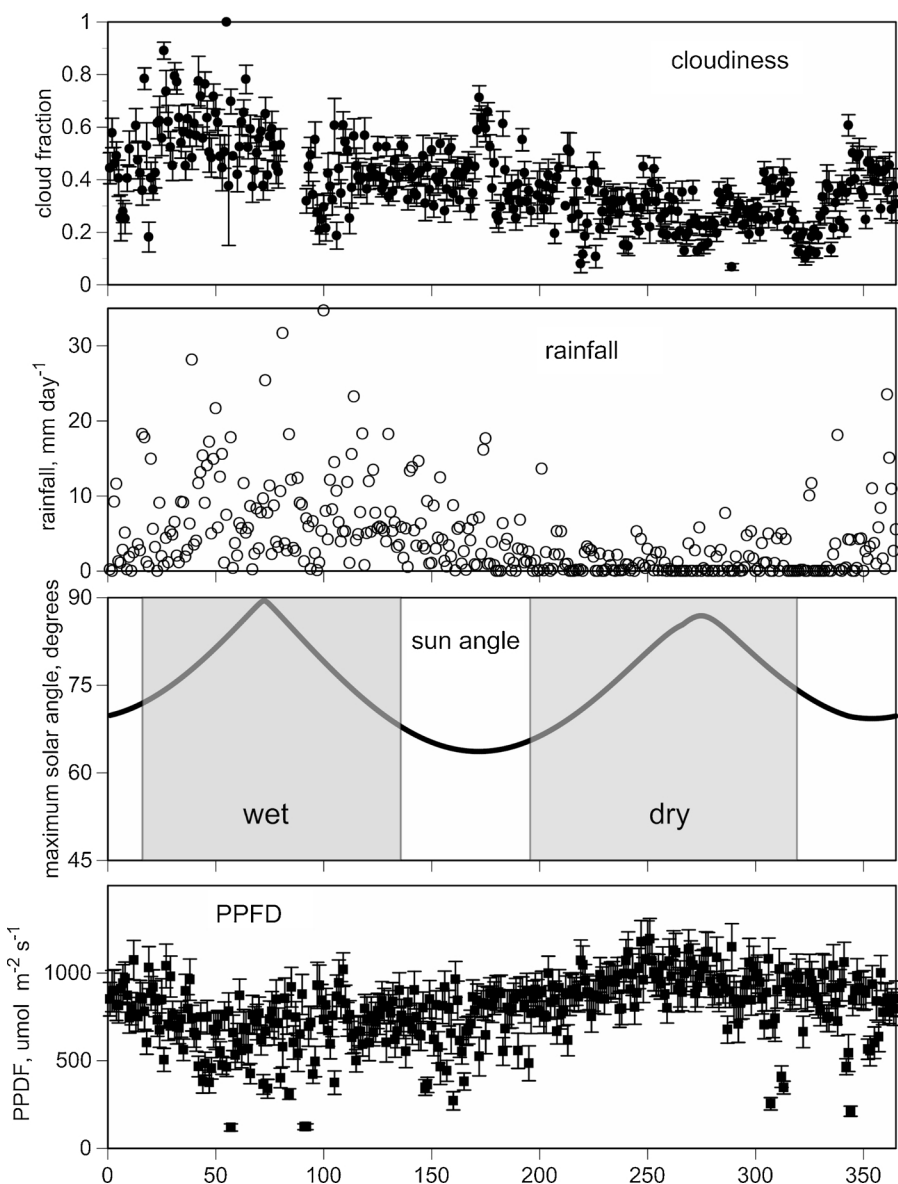


Fig. 2. Annual variation of atmospheric conditions at km67 for April 2001- June 2003. From the top, the panels show the mean day-time cloudiness, rainfall, maximum solar elevation angle and incoming PPFD for each day of the year. The error bars are standard errors. The seasons defined here are indicated as shaded regions in the solar elevation angle panel. There are gaps in the cloudiness observations on days 11–12, 59, and 81–91.

at 0.1 mm resolution every minute. At km67, all radiation measurements and the ceilometer observations were recorded on the same time base by a single computer using GMT (local time = GMT – 3).

2.2.1. Atmospheric transmissivity

Extraterrestrial radiation (PPFD_{ex}) was estimated with the [Spitters et al. \(1986\)](#) relation that depends on both solar elevation and day of the year. We define an index of sky “brightness,” the ratio of actual incident radiation (PPFD_{dw}) to that expected under clear sky conditions, PPFD_{max} . This measure is distinct from the clearness index [k_t], a ratio of global solar radiation at the ground to the corresponding extraterrestrial value ([Iqbal, 1983](#)). Our ‘brightness’ index (B) is:

$$B = \text{PPFD}_{\text{dw}} / \text{PPFD}_{\text{max}}$$

where PPFD_{max} is a sinusoidal function of solar elevation angle el (estimated with the algorithm of [Walraven \(1978\)](#) with corrections of [Walraven \(1979\)](#) and [Wilkinson \(1981\)](#)). [Brown et al. \(1994\)](#) used a similar approach. Maximal radiation values were identified as the 99th percentile observed for each 1° of solar angle. The resulting equation is

$$\text{PPFD}_{\text{max}} = 2034.8 \cdot \sin(el)^{1.0378}.$$

The function permits the detection of the occasional short-term but unusually high values of PPFD due to reflections from tall clouds. Note also that the brightness index (B) aggregates the contributing components of clouds, precipitation, dust, smoke, aerosols, water vapor and other sources that limit atmospheric transmissivity. This measure varies with but is not equivalent to, the sky diffuse fraction. Using this index, we define several brightness categories: I (< 30% of potential), II (30–60%), III (> 60–90%), and IV (> 90%).

2.3. Atmospheric environment

Pronounced dry and rainy seasons characterize the dominant seasonal atmospheric environment in the Tapajós National forest (see also [Goulden et al., 2004](#) for an earlier period). Solar input is greatest in the dry season when cloudiness is low and is least in the wet season when cloudiness is higher, even though the maximum sun elevations are somewhat higher in the wet season ([Fig. 2](#)). Solar elevation angles do

not exceed 64° during the transition seasons. The pattern of mean daily rainfall corresponds to the variation of daytime cloudiness ($r = 0.41$).

2.4. Seasonal differences in incident light environment

The importance of the atmospheric environment for forest PPFD interactions is clear from this study. Sky conditions control the quantity, quality and timing of light subsequently disposed in the ecosystem. The TNF lies in a region where cloudiness and rainfall are influenced by the Tapajós and Amazon river breezes during the day but also exhibit a nocturnal rainfall peak owing to the passage of long-lived squall lines that propagate in from the coast at this longitude (Fitzjarrald et al., 2008; Cohen et al., 2014). This affects the seasonal difference in the diurnal variation of cloudiness and rainfall that modulates incoming PPF_{dw}.

2.5. Understory radiation measurements

In the understory about 127 m ESE of the tower base we installed an array of light sensors in the shape of a nested pentagon: a centrally located PAR sensor and adjacent (2 cm separation between centers) pyranometer (LI-200SA, LI-COR, 2005) surrounded by 15 pyranometers with a 7.5 m spacing (range 7.5–28.5 m, 13.8 ± 7.8 mean separation, Fig. 3). The sensors were all intercalibrated in an open space before deployment in the understory. The array is located near the nocturnal CO₂ drainage study of Tóta et al. (2008), referred to as 'DRAINo'. Measurements at the array began 15 April 2002 (day 140) and continued through 4 June 2004 (day 156). A small gap was observed over the positions of sensors 4 and 11 when the array was installed. Radiation values at each sensor were sampled and recorded every ten seconds, on a common time base and with the same data acquisition system used for the above-canopy observations.

2.6. Spatial variation in PPFD transmission

To quantify the variability at scales both smaller and larger than those provided by the fixed array, we measured understory PPFD with a hand-carried TRAC system (3rd Wave Engineering, Nepean, Ontario, Canada) in three 1000 m transects extending to the NE, E, and SE of the tower (see Fig. 1 in Rice et al., 2004). TRAC data were recorded at 32 Hz from LI-190S quantum sensors oriented both facing up and down (Chen, 1996). The TRAC system was carried along transects, kept level using an aligned bubble level, with the reference plane at 1 m above the forest floor, at a speed of about 1 m s⁻¹. These larger-scale observations were taken twice in each of the wet and dry seasons, all under conditions including those with occasional clouds. Only on the dry season sample dates were all three transects acquired – each of the wet season dates had only one. As differences between seasons were small, we limit attention to the larger dry season dataset.

The ratio of the down-welling light at 1 m to the concurrent external value is termed "understory transmittance," T_{r1} . We assumed the external values were constant during the transects. The upwelling:downwelling ratio at this level (one sensor pointed up and the other down) is termed the "ground reflectance," R_g (see Parker et al., 2005). The ground reflection flux is the product of the understory transmission and ground reflectance, i.e., $PPFD_{gref} = PPFD_1 \cdot R_g$. Accordingly, ground absorbance is $PPFD_{gabs} = PPFD_1 \cdot (1 - R_g)$.

The spatial dependence of understory PPFD observations was evaluated differently for the two sorts of sampling schemes. For the long transects we calculated the autocorrelation for each sampling occasion and averaged these coefficients by 0.1 m groups. For the understory array, we calculated the correlation coefficient of the 0.1 Hz observations across all unique sensor pairs, for each season.

2.7. Data continuity, screening, and calibration

We first identified understory sensors having complete days of 10-s data. For these we subtracted the mean nocturnal noise level for each sensor and date. Silicon photovoltaic pyranometers are intended for natural daylight conditions (Jones et al., 2003, LICOR 2005, Mizoguchi et al., 2010). Accordingly, we calibrated the central pyranometer to the adjacent quantum sensor (the two diffuser tips were separated by 2 cm) with a reduced major axis regression (Sokal and Rohlf, 1995). The calibration function includes contributions of both the shade (umbral and penumbral) and sun-fleck (beam) phases. All pyranometer observations were then adjusted to yield PPF_D estimates. Pyranometer #10 failed early in the project and was excluded from all analyses.

We estimated missing values of incoming PPF_D from the nearby pasture site at km77 (Sakai et al., 2004). For three days with no data at either site we interpolated values from adjacent dates. We formed half-hourly averages of PPF_D for incoming (PPF_{dw}), reflected (PPF_{up}), and transmitting PPF_D (PPF₁) using the data from the up- and down-pointing exterior PPF_D sensors and the calibrated understory array. For each atmospheric brightness category, we constructed functions to estimate canopy reflection and transmission based on actual incoming radiation. The patterns for reflection were described with quadratic functions whereas those for transmission, which had distinctly greater curvature, required cubic functions. Using these functions, we then estimate canopy reflection, transmission to the understory, and canopy absorption ($= PPFD_{dw} - PPFD_{up} - PPFD_1 + PPFD_{gref}$) for each half-hour interval. This dataset was then used to produce budgets of all PPF_D components on daily, seasonal, and annual scales. We use the terms reflection, transmission and absorption in referring to flux densities, PPF_D. Reflectance, transmittance and absorbance denote the fraction of incident radiation with these particular fates. The reference level for understory observations and summaries is 1 m above ground.

2.8. Canopy reflectance and derived indices

The shortwave (S_{ref}) and PPF_D reflectances ($PPFD_{ref}$) are given as S_{up} / S_{dw} and $PPFD_{up} / PPFD_{dw}$, respectively. Up-welling and down-

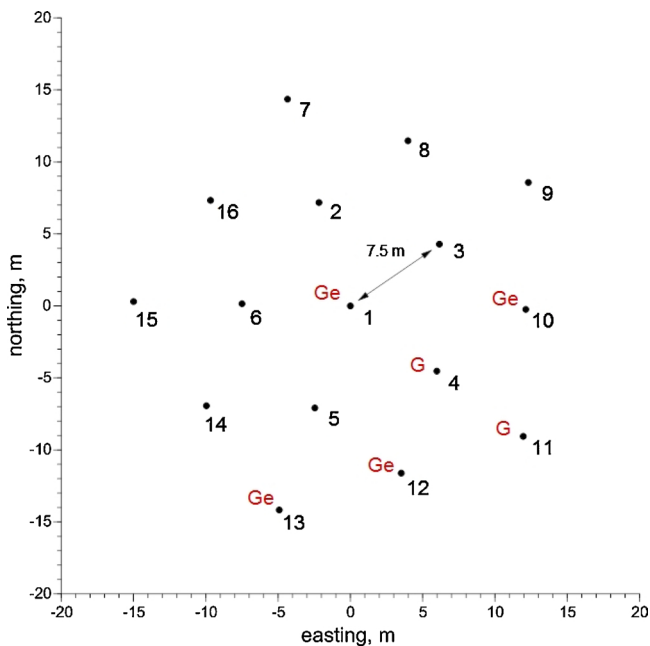


Fig. 3. Understory pentagonal array of light sensors at the base of the km 67 tower, sampled at 15 s intervals. Codes next to the numbered sensors indicate canopy conditions overhead observed at the installation of the array (G = gap, Ge = gap edge). Distances between sensor pairs ranged from 7.5 to 28.5 m.

welling components of the NIR band are estimated from the difference between the shortwave and PAR fluxes, when converted to comparable units using the factor c ($= 0.217$), the average conversion from quantum to energy units over the PAR waveband, similar to the value used by Thimijian and Heins (1983) for clear days.

$$\text{NIR}_{\text{ref}} = (S_{\text{up}} - c \cdot \text{PPFD}_{\text{up}}) / (S_{\text{dw}} - c \cdot \text{PPFD}_{\text{dw}}).$$

We calculated an approximation to the Normalized Difference Vegetation Index used in remote sensing to assess vegetation quantity and quality (Sellers, 1985; Myneni 1995; Moore et al., 1996; Huemmrich et al., 1999; Xiao et al., 2005; Huete et al., 2006). This index, the composite broadband NDVI (cbNDVI), is defined as:

$$\text{cbNDVI} = (\text{NIR}_{\text{ref}} - \text{PPFD}_{\text{ref}}) / (\text{NIR}_{\text{ref}} + \text{PPFD}_{\text{ref}})$$

2.9. Canopy structure measurements

Total surface area. We estimated the total canopy surface area per unit ground area, primarily consisting of leaves (here termed the Leaf Area Index, LAI) by combining our observations of understory transmittance with the algorithm of a commonly used commercial instrument, the LAI-2000 (LI-COR, 1992). As implemented, that approach estimates LAI as a weighted sum of transmittance measurements from different solar angle bands (Miller, 1967; Lang, 1986, 1987) under diffuse conditions. We used the half-hourly mean observations, restricted to conditions of most diffuse light (brightness classes I and II, Table 1). Comparable LAI estimates were not possible using this method during the transition season because the sun angles never rose to the 0–13° zenith angle of the LAI-2000 ‘Ring 1.’ The estimate we employ here, $5.05 \text{ m}^2 \text{ m}^{-2}$, is a spatial and half-hourly composite for low brightness conditions (I and II).

Vertical organization. We used an upward-facing high-frequency near-infrared laser rangefinder to provide metrics of canopy structure. The Portable Canopy LIDAR (PCL, described by Parker et al., 2004a) was carried along transects, held horizontally with the reference plane at 1 m. Observations were made in the dry season of 2004 in each of the three 1000 m long transects radiating upwind of the tower as well as in the DRAINO study area close to the understory array. Leitold (2009) repeated our measurements during the 2008 dry season and reported similar results. The metrics we derived, including the mean vertical distribution of surfaces (the Canopy Height Profile, CHP), the Local Outer Canopy Height (LOCH), canopy rugosity (standard deviation of LOCH), the cumulative frequency distribution of the outermost canopy heights, the hypsography (Pike and Wilson, 1971; Tarboton et al., 1989), are all derived with 2 m horizontal resolution. The size distribution of intercepted zenithal openings (the Gap Size Distribution, GSD) had a horizontal resolution of 0.033 m. These metrics and others employed are described by Parker and Russ (2004) and Parker et al. (2004a).

Canopy structure observations were conducted both around the tower, at the subcanopy CO₂ advection study area (‘DRAINO’; details in Tóta et al., 2008), and along the three 1000 m transects. The maximum surface height, mean LOCH, and the canopy rugosity are similar (Table 1). Further, the mean canopy gap fraction and the shapes of the GSD and CHPs are nearly identical (Fig. 4). The hypsographs (not shown) are similar among sites (two-sample Kolmogorov-Smirnov test, $p < 0.01$). Our measured gap size (Table 2) (1.2–1.4%) is similar to that reported by Espírito-Santo et al. (2014), who studied the nearby km83 Tapajós forest site. Because of these similarities in canopy structure, we treat our intensive observations in the array area as generally representative of the km67 flux footprint.

Within-canopy light environment We estimated the vertical distribution of spatially-average PAR transmission and absorption by application of the Beer-Lambert law based on the mean CHP. For each 0.5 h period, we calculate the transmittance to the understory, Tr_1 , as:

$$Tr_1 = \text{PPFD}_1 / (\text{PPFD}_{\text{dw}} - \text{PPFD}_{\text{ref}})$$

Then we calculated the bulk extinction coefficient, k_{bulk} :

$$k_{\text{bulk}} = -\ln(Tr_1)/\text{LAI}$$

using the annual average LAI of 5.05 derived as described previously. With this extinction coefficient, we calculated the PPFD for each canopy level (PPFD_h):

$$\text{PPFD}_h = (\text{PPFD}_{\text{dw}} - \text{PPFD}_{\text{ref}}) \cdot \exp(-k_{\text{bulk}} \cdot \text{LAI}_h)$$

where LAI_h is the cumulative LAI from the canopy top to height h. Note that we use the difference between PPFD_{dw} and PPFD_{ref} to estimate the incoming PPFD to be distributed within the canopy.

Assuming negligible within-canopy scattering, the PPFD absorption in a layer of canopy, ABS_h, may be estimated as the difference in transmission between levels:

$$\text{ABS}_h = \text{PPFD}_{h+1} - \text{PPFD}_h$$

Because of the temporal variations in PPFD_{dw}, PPFD_{ref}, and PPFD₁, the quantities k_{bulk} , PPFD_h, and ABS_h were calculated for every half-hour period from the canopy top to $h = 1$.

We used calibrated but un-averaged data to construct the prediction functions, for the canopy reflective index, and for the assessments of understory PPFD frequency, duration and spatial-temporal patterns. For budget accounting, we used a composited dataset that included some external fluxes estimates from similar observations at nearby sites. The close comparison in estimates – for example, for PPFD_{up} the estimates and actual values are within 0.3% – gives confidence in the estimating procedure. The period we report for the annual budget ran from 17 July 2002 (day 198) through 16 July 2003 (day 197). We used the SAS package (SAS Inc., 2008) to organize the data and perform statistical analyses.

3. Results

3.1. Clouds, rain and sky brightness

Sky conditions strongly influence the observed radiative behaviors of the atmosphere, canopy surface and full canopy. For example, just before and after the passage of tall cumulus clouds we often observed PPFD in the 5-s data well in excess of that expected. On the basis of half-hour data, we found atmospheric transmittance (brightness) to be primarily influenced by solar elevation ($r = -0.26$) and cloudiness ($r = -0.31$) on an annual basis. Canopy reflectance is primarily controlled by cloudiness ($r = -0.20$) and, to some extent, solar elevation ($r = -0.19$); sky brightness had relatively little effect ($r = 0.06$) on canopy reflectance. In the case of canopy transmittance, the main influence was solar elevation ($r = 0.66$), although brightness ($r = 0.03$) and cloudiness ($r = 0.16$) were also factors. PPFD_{dw} was affected by cloudiness ($r = -0.18$) but not by rain. Canopy-absorbed PPFD was strongly related to solar elevation ($r = 0.77$) and brightness ($r = 0.77$) but only somewhat to cloudiness ($r = -0.18$) and not to rain.

Table 1

Estimates of canopy Leaf Area Index (LAI) using radiation measurements from this study and the algorithm employed by the LAI-2000 instrument. The all-seasons estimate for brightness classes I and II is used in this study.

| Brightness | Season dry | wet | all |
|------------|---------------|------|------|
| I and II | 5.02 | 5.05 | 5.05 |
| III and IV | 4.98 | 5.06 | 5.00 |
| all | 4.98 | 5.04 | 5.00 |

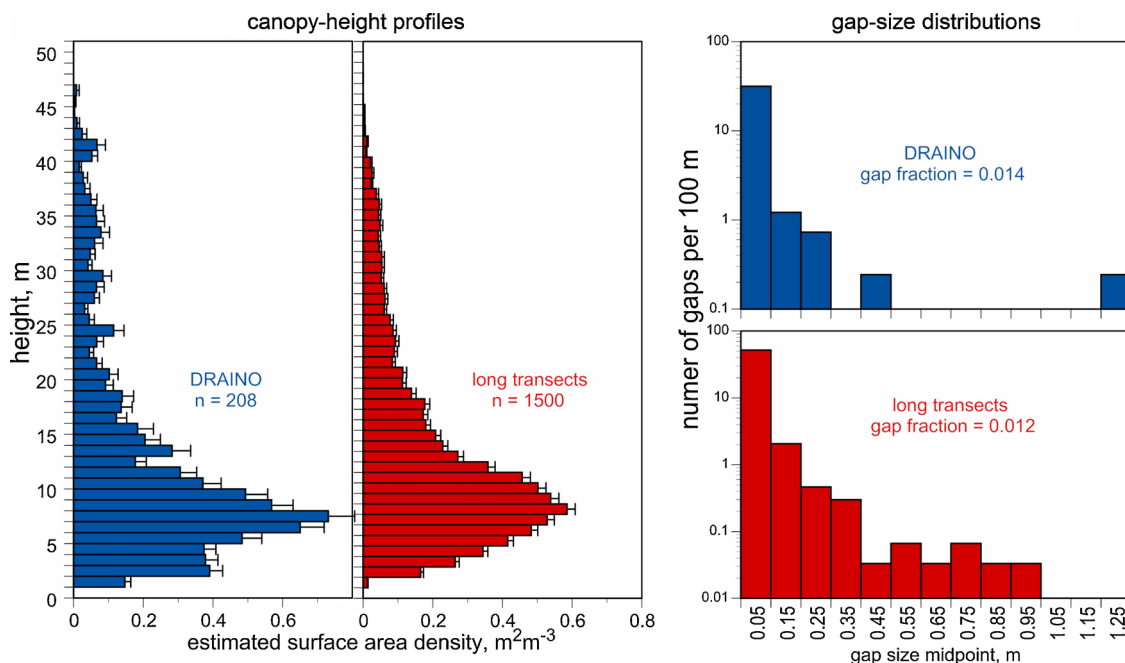


Fig. 4. Canopy structural metrics derived from ground-based LIDAR for the DRAINo area very close to the understory array and the intensive sampling area 1000 m upwind of the km67 tower ('long transects'). The leftmost panels compare the Canopy Height Profiles (CHP); the panels on the right contrast the size distributions of zenithal openings (GSD).

Table 2

Comparison of canopy structural attributes between the subcanopy advection study (Tóta et al., 2008) area near the understory sensor array (208 m total transect length) and the three 1000 m 'footprint' transects. Rugosity is the standard deviation of the mean canopy height.

| Structural characteristic | Study area | |
|------------------------------|-------------|----------------|
| | DRAINo area | long transects |
| mean outer canopy height (m) | 19.6 | 20.1 |
| outer rugosity (m) | 11.4 | 10.03 |
| 99th percentile height (m) | 43.5 | 43.5 |
| total openness fraction | 0.0142 | 0.0119 |

3.2. Predicting canopy reflection and transmission

Canopy reflection in the PAR spectral region is a nearly constant fraction of incoming light (2.0% of PPFD_{dw}) (Fig. 5, left panel) with little effect of sky brightness. The relation is slightly convex, which corresponds to somewhat higher reflectance (around 2.5%) at sun angles less than 10°. In contrast, canopy transmission (Fig. 5, right panel) is not only non-linearly related to incident PPFD but also is markedly affected by sky brightness. The greater transmission under diffuse conditions compared to bright ones is especially evident where PPFD is less than 600 μmol m² s⁻¹. Transmittance suggested by Fig. 5 is about 6.5% for brightness class I and around 3.0% for class IV. At much higher levels (greater than 1200 μmol m² s⁻¹), transmittance for brightness classes III and IV can range as high as 9.5%.

3.3. Frequency of occurrence of understory light flux

The frequency distribution of understory PPFD was extremely steep, with a longer tail than a lognormal distribution has (Fig. 6). Overall, 32.6% of observations exceeded 50 μmol m² s⁻¹, a common threshold definition for sun-flecks (e.g., Chazdon, 1988); 39.7% were of sun-fleck intensity in the dry season and 17.2% in the wet. The frequency of higher levels also differed among seasons – 2.42% of all dry season values exceeded 200 μmol m² s⁻¹ compared to 0.68% during the wet

season. The maximum of the total quantum flux (i.e., the product of the category value and the number of observations) occurred in the 40–50 PPFD range. Note the increase in the dry-season distribution apparent near 1500 μmol m² s⁻¹. This was due to a transient gap above sensors 4 and 11 (Fig. 3), where higher values were observed early in the study. When depicted as the fraction of observations exceeding a PPFD level (Fig. 6 inset), the distribution appears to be composed of two linear segments that intersect near 200 μmol m² s⁻¹. This intersection might indicate a change in the light regime, from predominantly shade light to mostly sun-flecks.

3.4. Duration of understory light intensities

As expected, darker conditions are more persistent than are brighter ones. In Fig. 7, it is clear that the overall relation between intensity and duration is negative and strongly curvilinear. Durations are highly positively skewed (skewness coefficients exceeded 5.0 for all levels.) The median duration declined from 80 s at low light to 20 s in brighter conditions. Light levels below 50 μmol m⁻² s⁻¹ last on average 341 s (5.7 min). By contrast, light levels of 200 μmol m² s⁻¹ or more rarely continue longer than 62 s (1.0 min). The mean duration of higher levels is essentially constant, indicating the influence of occasional very bright sun-flecks. Note the dry season asymptote is higher than that of other seasons, reflecting the influence of a transient gap in the canopy above two sensors. The inset figure shows this distribution for locations in a transient gap (sensor 11) and in persistent shade (sensor 1).

3.5. Spatial and temporal association of understory transmittance

Observations from both fixed temporal/varying spatial and fixed spatial/varying temporal sampling schemes showed the spatial covariance of understory PPFD declined very steeply at near distances, such that at 10 m between sensors the autocorrelation averaged 0.3. The pairwise correlation between sensors at the fixed sensors was essentially flat ($r^2 = 0.10$, not significant) at distances across the scale of the array (7.5–28.5 m) in all seasons. Absolute correlations (not shown) were somewhat higher in the dry season than in the wet.

The shape of the understory light field for a 100-day period in the

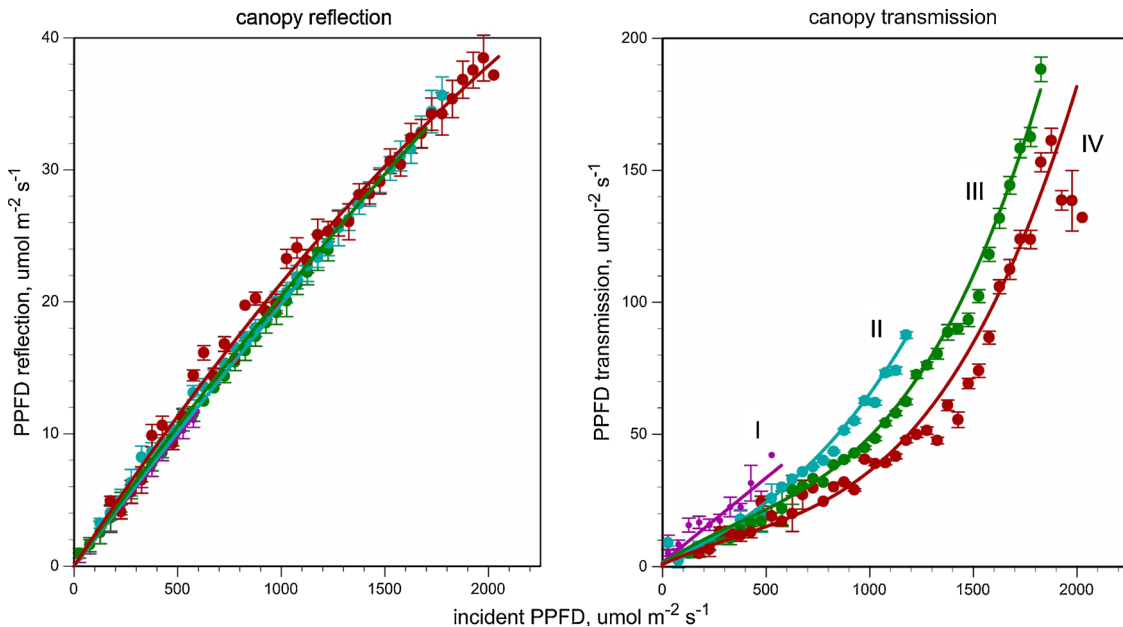


Fig. 5. Canopy PPFD reflection (left panel) and transmission (right panel) with incoming PFD for each of four sky brightness categories (I-IV). The lines fitted for each radiation component and brightness level are described in the text.

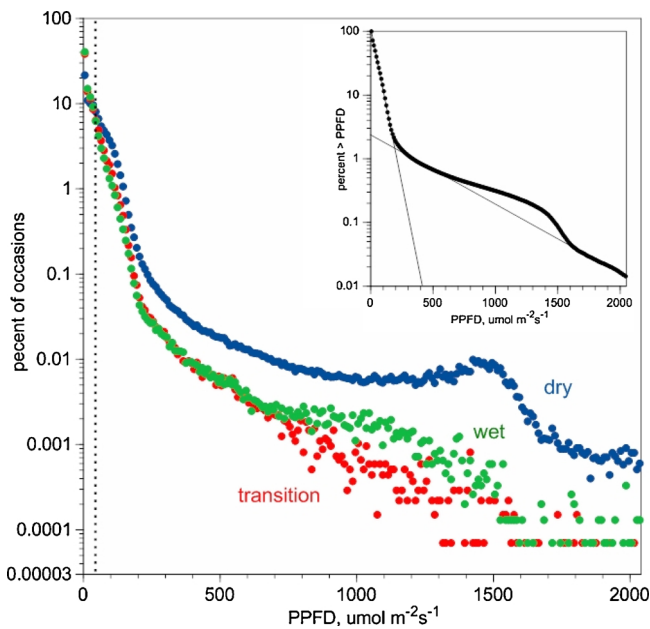


Fig. 6. Frequency distribution of 10-s understory observations of PPFD in each season (colored symbols). The dotted vertical line, at $50 \mu\text{mol m}^{-2} \text{s}^{-1}$, is the sun-fleck threshold. The inset panel shows the percentage of all observations exceeding a PPFD level. Note the two relatively linear segments, indicated with faint lines. The ordinate axes in both panels are logarithmic.

middle of the dry season, when there was relatively few completely overcast periods, shows dark and bright locales that vary slowly in time (Fig. 8). Note the slow migration of a bright area from the SE corner of the network to the center and then to the NE, indicating the changing and directional geometrical relationship between canopy features and sun angle. The maximum sun angle during this period changed from 67.5° (day 206) to a peak of 88.7° (270), declining again to 77.1° (306). The mean pattern for this interval (Fig. 8, lower right panel) is dominated by the effects of the transient gap above sensors 4 and 11. Correlations are high for day-to-day changes ($r = 0.89$) but decline progressively ($r = 0.74$ at one week, $r = 0.42$ after four weeks).

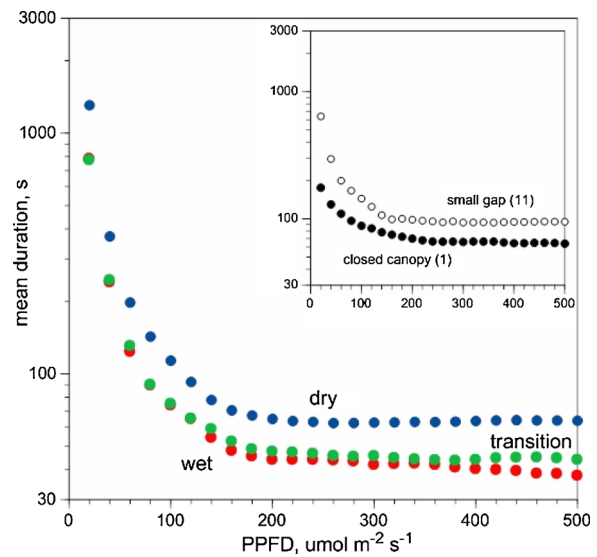


Fig. 7. Frequency distribution of the duration of daytime understory PPFD of different levels for each season. The inset figure shows this distribution for locations in a transient gap (sensor 11) and in persistent shade (sensor 1).

3.6. Daily variation in understory transmission

The spatial median transmission of PPFD to the understory is symmetrical about the time of solar noon in all seasons and for the year combined (Fig. 9). Transmission is higher than the annual average in the dry season and less during the wet and transition seasons, following the seasonal differences in incoming PPFD. Note that lowest levels of understory light (5th percentile line, Fig. 9) can reach $52 \mu\text{mol m}^{-2} \text{s}^{-1}$ in the dry season and even $26 \mu\text{mol m}^{-2} \text{s}^{-1}$ in the wet season.

There were location-specific differences in the amounts and diurnal pattern of understory transmission (Fig. 10). Unlike the pattern for the array average (Fig. 9), the daily patterns for the individual sensors were sometimes asymmetrical – for example, sensors 11 and 16 had pronounced afternoon maxima not exhibited at other locations. Note also the higher mean levels at sensors 4 and 11, reflecting of the transient gap.

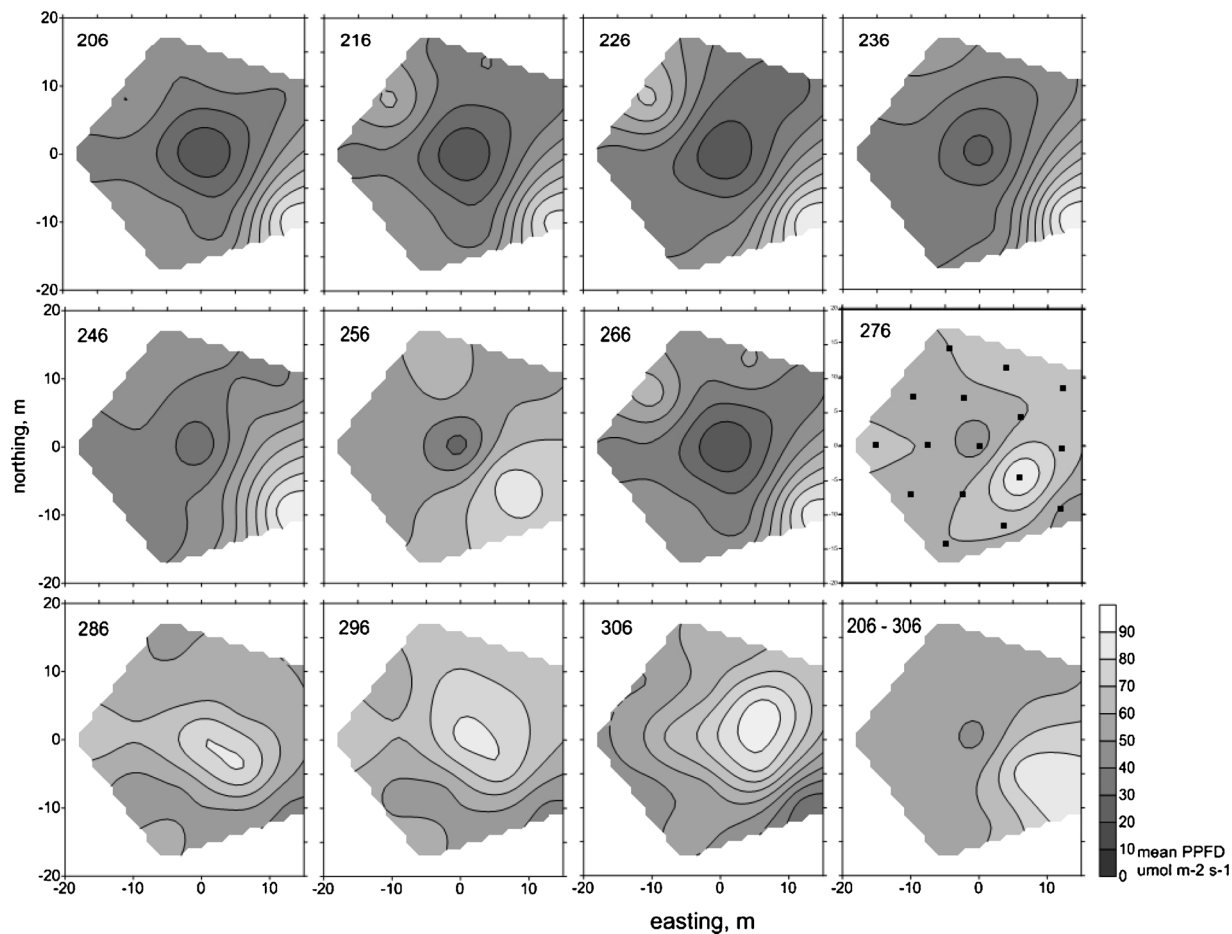


Fig. 8. Spatial pattern of mean daily understory PPFD for a series of dates (numbered on each panel) in a 100-day period in the dry season. While the range of PPFD varies by date, in each plot the darkest shading indicates values from 0 to $10 \mu\text{mol m}^{-2} \text{s}^{-1}$; the contour intervals are separated by $10 \mu\text{mol m}^{-2} \text{s}^{-1}$. The arrangement of the array sensors relative to the PPFD field is indicated in the plot for day 276. The contour scale refers to the mean pattern for the period given in the lower right panel.

3.7. Daily march of canopy reflectance, transmittance, and the extinction coefficient

There is little diurnal change in PPFD reflectance in any season, except for some increase at low sun angles. However, mean transmittance changes dramatically over the day, nearly doubling from morning or evening to mid-day. Seasonal variations in transmittance differ somewhat from the corresponding patterns of transmission (Fig. 9) because of seasonal variation in PPFD_{dw} .

The extinction coefficient for canopy transmittance ($k = -\ln(\text{Tr}_1)/\text{LAI}$) changes diurnally – it is highest in the morning and afternoon but relatively stable within two hours of solar noon. As expected, this pattern is partly due to the change in length of the canopy path through which PPFD must pass.

3.8. Canopy vertical distribution of PPFD transmission and absorption

Seasonal patterns in the mean vertical profiles of PPFD (Fig. 11, left) and absorption (Fig. 11, right) are similar in shape but differ in scale. The vertical gradient of PPFD is low in the both the outermost canopy (40–50 m) and in the layers near the forest floor (1–5 m) – the steepest gradient in transmitting PPFD is between 8–19 m, the height range of greatest PPFD absorption (Fig. 11, right).

Diurnally, however, the vertical patterns of PPFD transmission and absorption (essentially the vertical derivative of transmission) vary distinctly. For example, the vertical gradient in transmission is slight before 11.0 and after 20.0 GMT; very little PPFD arrives at the ground

at these times. The gradient steepens progressively with increasing sun angle and the greatest transmission to the whole canopy occurs around solar noon. Most all absorption occurs at canopy heights between 8–19 m and times between 12.5–18.5 GMT. Despite the tall stature of the forest, most of the PPFD interaction occurs in the lower canopy.

3.9. Canopy reflectance and a vegetation index

The effect of solar elevation angle on the measured reflectance of total solar radiation (S), PPFD and the derived NIR reflectance and composite NDVI is shown in Appendix A. for elevations greater than 5 degrees and the clearest skies (brightness classes III and IV, with greater than 60% of potential light PPFD_{max}). The annual mean reflectances of the PPFD, S and derived NIR bands are 2.0, 12.5 and 18.1%, respectively. The angle dependence of reflectance is a not a strong characteristic of PPFD but it is for the total shortwave (S), and especially for the near-infrared, NIR. The composite broadband NDVI also varies with solar angle, perhaps accounting for the observation of seasonal variation in such indices in studies of high- and mid- latitude forests (e.g., Huemmrich et al., 1999; Moore et al., 1996). The cbNDVI is slightly higher in the dry (0.791 ± 0.003) than in the wet season (0.823 ± 0.002), with solar elevation $> 40^\circ$, a small but significant difference, owing to the large number of cases.

3.10. Forest PPFD budget

On an annual basis, the incoming PPFD is reduced by canopy

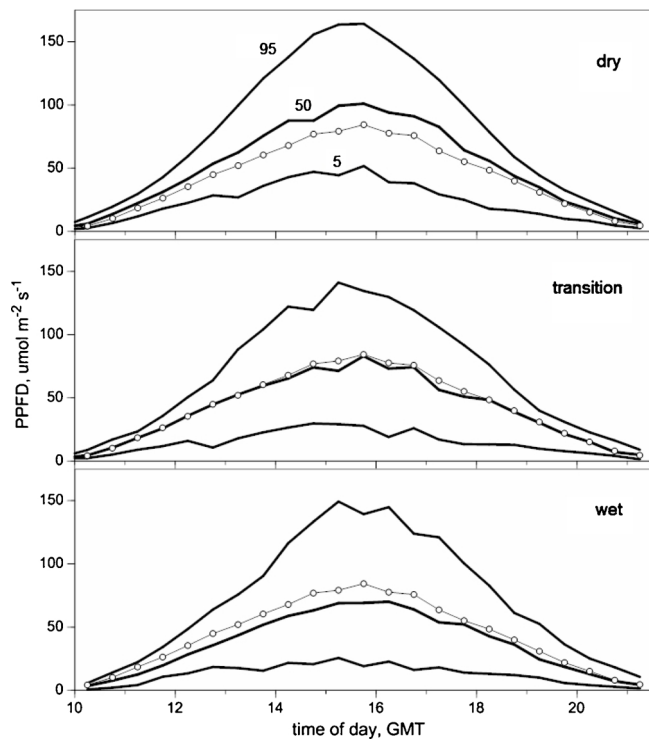


Fig. 9. Seasonal variation in understory transmission. The pattern of half-hourly PPFD for all sensors for the dry (top panel), transition (middle) and wet (lower) seasons are given by symbols connected with bold lines. In each panel the central line is the median - the upper and lower are the 95th and 5th percentiles. The annual median pattern is given in each panel by a line with open symbols.

reflection (2.01%) and absorption by the forest floor (5.58%) – the majority (92.4%) is absorbed by the canopy (Table 3). A very small portion of that absorption is from ground reflection (0.16%). Consequently, transmittance is about 5.74%.

Seasonal and daily variation in the radiation budget. The annual variation in potential and actual PPFD input is controlled by seasonal patterns in sun angle and sky conditions. Factors affecting atmospheric transmissivity and their seasonal variation are important in the km67

light environment – the dry season had more potential radiation (69.9%) than did the wet season (52.1%). The actual annual PPFD input ($11,795 \text{ mol m}^{-2}$) is only 61.6% of the potential amount under clear skies. Potential clear-day PPFD was a nearly constant fraction (72.3%, ranging 71.9–72.9% seasonally) of the concurrent extraterrestrial flux.

Diurnal and seasonal variations in these proportions depend closely on atmospheric conditions affecting PPFD_{dw} . When there is less light due to reduced atmospheric transmissivity or low sun angles, less is reflected or penetrated. However, the proportional disposition of radiation components remains about the same. In the wet season, the transmission to the understory was 42.2% greater than in the dry (Table 3) but transmittance was only 3.0% greater (5.9% in the dry season compared to 5.7% in the wet season).

The components of the PPFD budget also vary seasonally. While the potential incoming flux (PPFD_{max}) varies little by season, all other components follow the change in incoming radiation (PPFD_{dw}), which is affected by sky conditions (Table 4). Consequently, both the absorption (APAR) and canopy transmission are greatest in the dry season.

4. Discussion

Our study combined many ways of observing light in forests. We measured transmission over a long term in a small area and over a short-term over a much wider area with high frequency samples. We derived the long-term coarse angular distribution of transmittance at one site and zenithal variation of canopy openness over a large area. With near-infrared laser light we measured the distance to canopy surfaces and used the derived canopy structure to estimate vertical patterns of canopy transmission.

Reflection and transmission. Our predictors of major radiation components were strong functions of PPFD_{dw} . PPFD reflection (PPFD_{up}) was relatively insensitive to sky brightness (i.e., the four brightness curves were nearly collinear). Unlike the reflectance functions, those for transmission (PPFD_1) were markedly curved. The curvature depended on the brightness, becoming more pronounced with increasing brightness. This suggests that radiation interaction with canopy elements may depend on the intensity of PPFD_{dw} . This possibility is discussed below.

As we found, other studies in forests and other vegetation report that canopy reflection of PPFD is relatively low (0.03–0.07: Hassika and Berbigier, 1998; Huemmrich et al., 1999; Leitão et al., 2002; Parker

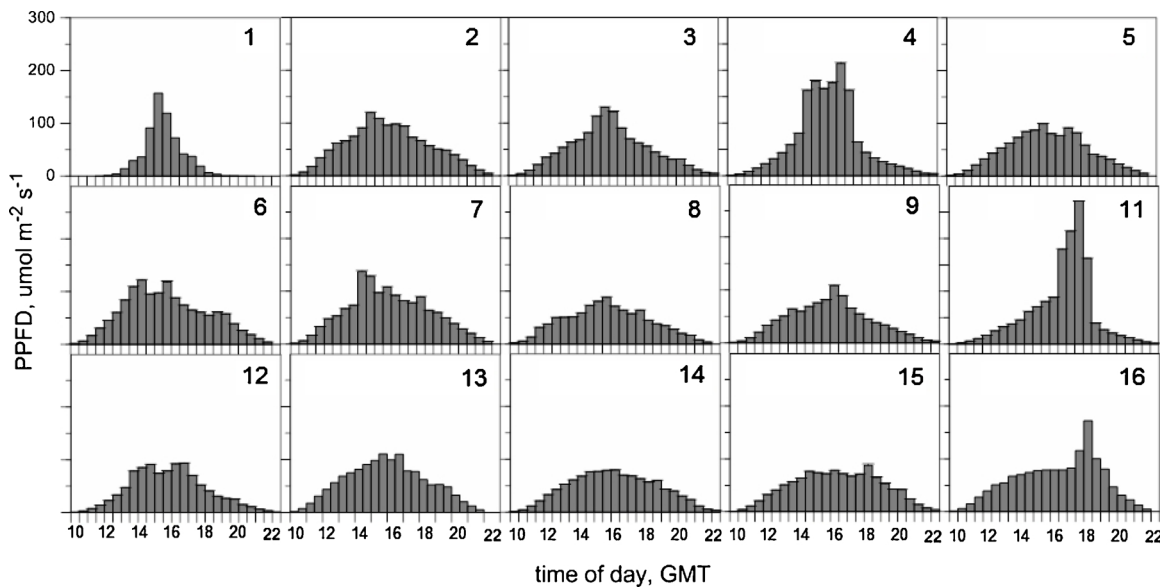


Fig. 10. Spatial variation of understory transmission. Each panel gives the annual mean PPFD for each half-hour period at the 16 locations in the sensor array. The sensor number is given in each panel (spatial arrangement in Fig. 4).

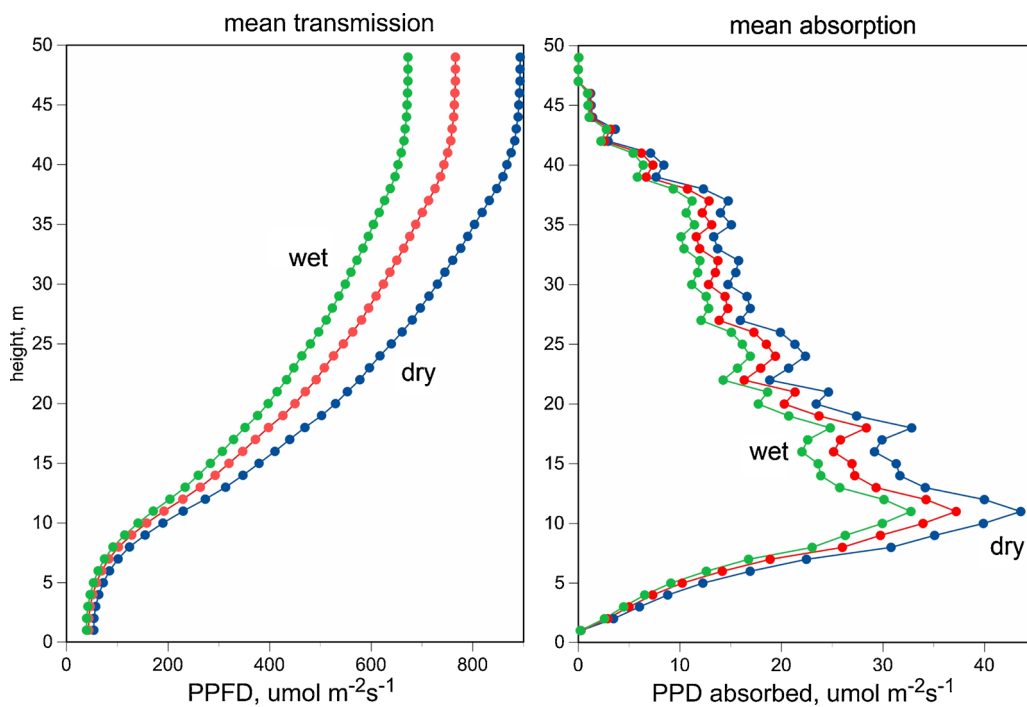


Fig. 11. Vertical pattern of light environment in the km67 forest canopy. The left panel gives the mean available PPFD (transmission) at each meter of height – the right panels give the change in transmission between a layer and the one above (absorption).

Table 3

Components of the PPFD budget, mol m⁻², for the forest canopy at the km67 site, by season and for a whole year.

| PPFD category | Season | | | |
|--------------------------------|--------|------------|------|--------|
| | dry | transition | wet | all |
| PPFD _{ex} | 9136 | 8344 | 9008 | 26488 |
| PPFD _{max} | 6663 | 6022 | 6473 | 19157 |
| PPFD _{dw} downwelling | 4659 | 3762 | 3374 | 11,795 |
| Canopy reflection | 94 | 76 | 68 | 237 |
| Canopy transmission | 275 | 209 | 193 | 677 |
| Ground reflection | 8 | 6 | 5 | 18 |
| Ground absorption | 267 | 204 | 188 | 658 |
| Total PPFD absorption | 4298 | 3482 | 3119 | 10899 |
| Duration, % of time | 34.4 | 32.4 | 33.1 | 99.9 |

Table 4

Components of the PPFD budget, mol m⁻², for the forest canopy at the km67 site, by sky brightness category.

| PPFD category | Brightness class | | | | |
|--------------------------------|------------------|------|-------|------|--------|
| | I | II | III | IV | All |
| PPFD _{ex} | 2942 | 8281 | 13141 | 2125 | 26488 |
| PPFD _{max} | 2115 | 5958 | 9548 | 1537 | 19157 |
| PPFD _{dw} downwelling | 394 | 2802 | 7141 | 1457 | 11,795 |
| Canopy reflection | 8 | 56 | 144 | 29 | 237 |
| Canopy transmission | 25 | 150 | 414 | 87 | 677 |
| Ground reflection | 1 | 4 | 11 | 2 | 18 |
| Ground absorption | 24 | 146 | 403 | 85 | 658 |
| Total PPFD absorption | 362 | 2600 | 6594 | 1343 | 10899 |
| Duration, % of time | 13.5 | 34.3 | 45.3 | 7.0 | 100.0 |

et al., 2005; Doughty and Goulden, 2008; Yoshimura and Yamashita, 2012). Reflection is often ignored in PPFD budgets (e.g., Gower et al., 1999). Other bands of short-wave radiation have distinctly higher reflectance (Barradas, 1991; Sugita and Kotoda, 1991; Barradas and Adem, 1992; Huemmrich et al., 1999; Leitão et al., 2002; Parker et al.,

2004b). The dependence of PAR reflectance on solar angle is also slight compared with that of other wavebands (Appendix A).

4.1. Understory light

4.1.1. Frequency and duration

As expected, transmitting PPFD is most often low in intensity and long in duration; higher levels are increasingly uncommon and brief. Ross and Möttus (2000) found a similar result, though they focused on the umbral phase. Our analysis suggests that an understory plant would be exposed to durations of PPFD that declined as the intensity rose. For example, Küppers et al. (1996) describe sun-fleck duration in various canopy environments in a Costa Rican forest. They found total daily light dose was in shorter duration sunflecks low in the canopy compared with gaps or higher sites. A representation such as given in Fig. 8 could be useful to estimate the regimes of changing light in the understory, especially for plants dependent on persistent sun-flecks (e.g., Young and Smith, 1979; Pearcy, 1990; Koizumi and Oshima, 1993; Naumburg and Ellsworth, 2000).

4.1.2. Spatial pattern of understory light

Estimates of the spatial scale of variation in understory light have been reported by Becker and Smith (1990); Smith et al. (1992); Clark et al. (1996); Walter and Grégoire, 1996; Trichon et al. (1998); Nicotra et al. (1999), and Wirth et al. (2001), but differences in methodologies, times of day, sky conditions, and methods of estimation make the derived scales difficult to compare. Our assessment of the spatial variation of understory PPFD is a combination of two sorts of observations: one type taken in a short period over a large spatial scale (transects acquired with the TRAC instrument) and another set taken simultaneously over a long time at a limited spatial scale (the array). This representation combines complementary long term, small-scale with occasional larger-scale observations, both at sub-minute frequencies. These complementary aspects of radiation spatial covariance provide support that our detailed local observations represent a larger region.

The correlations among locations at the array were on the order of $r = 0.3$; those of the TRAC samples ranged around $r = 0.1$ at the same

(7.5–28.5 m) spatial scale. Several factors may have contributed to this difference. The TRAC sampled over a large area (≈ 3000 m), covering a wider range on canopy structures than at the array, including many large canopy openings. A greater range in adjacent structure differences over the long transects would cause rapid declines in correlation; the canopy structure at the array was more uniform. Furthermore, the array values are averaged by half-hour periods, which will necessarily reduce the variance within and increase the correlation among sensors.

4.2. Canopy structure

Our estimation of LAI differs in several respects from the mode in which the LAI-2000 is typically deployed. The LAI-2000 acquires instantaneous observations of primarily blue light transmittance at different solar angle bands. Our estimate used occasions over many days and many locations when the sun disk was in that band – it sacrifices the simultaneous observation of transmittance at many angles, but allows spatial and temporal averaging that makes it more broadly representative. Our LAI estimate ($5.05 \text{ m}^2 \text{ m}^{-2}$) is indistinguishable from the $5.07 \pm 0.17 \text{ SE}$ annual mean reported by Malhado et al. (2009). It is in the range of other values reported from sites at or near km67 with similar methods (see the Williams et al., 1998 compilation). Domingues et al. (2005) acquired LAI-2000 derived estimates at various heights from several towers in the Tapajós area. Their Fig. 1 shows a nearly linear decline in ‘Cumulative LAI’ at km67 from the canopy top, with an estimated ground LAI of 4.47 (their Table 3). We found a similar estimate of total LAI but with a different vertical distribution. Rather than a linear accumulation from the top we found a steep decline of surface area density in the overstory with a pronounced understory peak (also reported by Leitold, 2009 and Stark et al., 2012 at this site). A possible cause of the difference between our results and those of Domingues et al. (2005) is due to sampling scales: our measure of vertical structure was taken over a large area (3000 m) whereas theirs was restricted to heights along the tower itself. Owing to the presence of the tower structure and the openness of the surrounding canopy, the Domingues et al. (2005) results may be less representative of the wide area.

4.3. Canopy structural influence

We estimate the mean transmittance profile using the Canopy Height Profile (CHP) derived using the Beer-Lambert law (Parker et al., 2004b) with LIDAR-based structure measures and a ground-based estimate of LAI. We have no independent direct measurements of vertical canopy PPFD for corroboration. The PPFD observations at 15 m at the tower reported by Senna et al. (2005), probably unrepresentative of canopy conditions, cannot yield a profile. Our method cannot yield vertical variations in transmission, as we have no long-term estimates of canopy structure corresponding to the understory transmittance observations. Horizontal variation in transmission can be significant within the canopy; for example, the spatially extensive study of vertical changes in PPFD transmission in a somewhat shorter stand in the Orinoco basin, Anhuf and Rollenbeck (2001) found high horizontal variation in transmittance (82.2% coefficient of variation, R. Rollenbeck, personal communication) in the middle canopy. It is unlikely that such variation can be captured at a single location.

We estimate a very gradual vertical change in transmission in the upper canopy. However, in the lower canopy the transmittance gradient ($\Delta \text{PPFD}/\Delta z$) is quite steep – substantial amounts of PPFD occur nearly to the understory. The maximum of PPFD absorption also occurs rather low, at between 8 and 19 m (29–46 % of canopy height, Table 2). This is also the height where the product of transmittance and leaf area density, the ‘solar equivalent leaf area’ is greatest (Čermák, 1989). This location of activity may appear counterintuitive given the tall stature of the km67 forest (canopy surfaces were observed as high as 50 m above ground, Fig. 4). However, this forest has a highly irregular outer surface; the LOCH at many locations extending to within 5 m of the ground

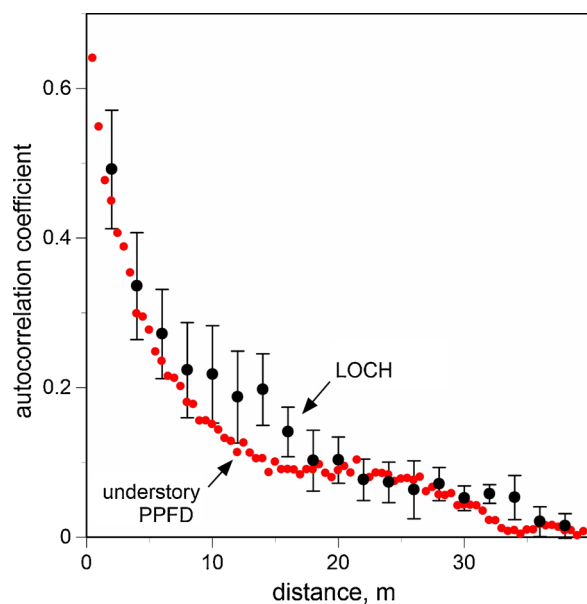


Fig. 12. Autocorrelation of both understory light and outer canopy structure taken along the three 1000-m transects. Group widths are 2.0 m for Local Outer Canopy Height (LOCH) and 0.5 m for PPFD, every fifth value plotted. Bars on the LOCH values are standard errors – errors bars are not shown for PPFD.

(Table 2). High rugosity is a common feature of old growth forests (e.g., Parker et al., 2002; Parker and Russ, 2004; Parker et al., 2004b). This aspect of the canopy structure is not always apparent at the ground, especially in tropical forest where cover is quickly re-established following opening of the canopy (e.g., Asner et al., 2004).

Our observations cannot specify which physical elements control the precipitous spatial decline in autocorrelation of understory PPFD. Transmittance (0.057 overall) is greater than the zenith gap fraction (0.012) – this suggests that the dominant canopy features controlling light environment are distributed over a range of angles above. Nonetheless, the similarities in the spatial dependence in LOCH and understory PPFD structure suggest it is likely some aspect of canopy structure within 10–20 m (Fig. 12), such as overstory crown size. Using IKONOS imagery Palace et al. (2008) estimated mean outer canopy crown width in the Tapajós region to be $13.1 \pm 0.1 \text{ m}$ (range: 2.0–38.0 m).

4.4. Comparing atmospheric and understory light environments

Two sequential filters. The chance that light will penetrate a medium is related to the concentration of absorbers along the beam path. This has long been recognized for the atmosphere (the Beer-Bouguer-Lambert law) and was subsequently modified for vegetation (by Monsi and Saeki, 1953), where the leaf area (LAI) was substituted for optical depth. This description works well in the atmosphere but is less apt for canopies. We illustrate this difference by comparing atmospheric and canopy properties at km67.

The flux of PPFD through the atmosphere, PPFD_{dw} , increases linearly with solar elevation ($r^2 = 0.996$, Fig. 13 top left). However, the flux of PPFD transmitting the canopy does not decline constantly with sun angle, but shows two regimes, with an abrupt change in slope at about 32° (Fig. 13 bottom right). Note that 32° elevation is nearly the same as the angle of 1 rad from the zenith recommended for LAI estimation by Lang (1987). Expressed in terms of fractional illumination, atmospheric transmittance rises progressively with sun elevation (Fig. 13 lower left). Canopy transmittance however, is relatively constant at low angles and rises with solar elevation at higher sun angles (Fig. 13 lower right). The canopy differs from the atmosphere in the character of absorbing surfaces and the resulting occlusion of light. Canopy transmittance may be pictured as operating in two regimes: at low sun angles the canopy acts

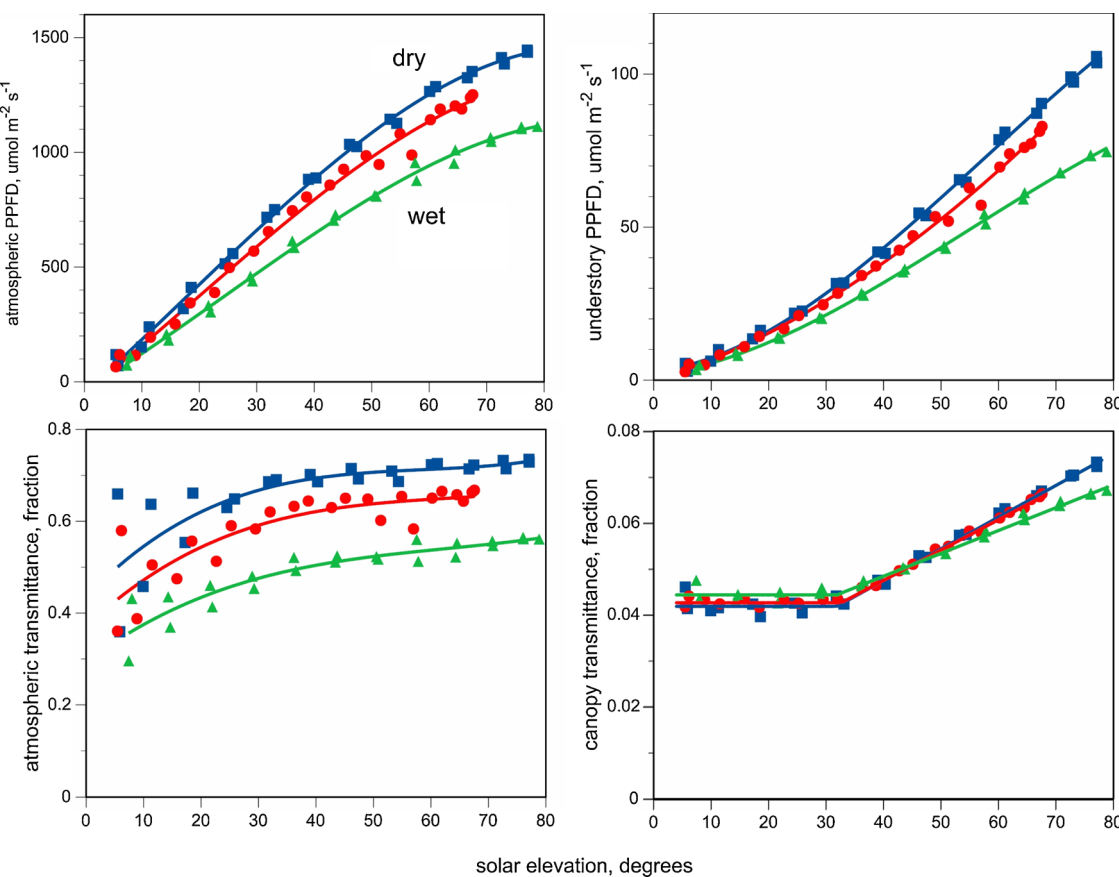


Fig. 13. Solar elevation-dependence of the atmosphere (left hand panels) and canopy (right hand) filters of PPFD. The top panels give the absolute PPFD (transmission) through the sky and canopy while the bottom panels exhibit the fractional passage (transmittance). The seasons are distinguished by color.

as a constant fraction filter, and at angles above a critical value it permits the passage of proportionally more photons as solar elevation increases. We propose that the low-angle regime is dominated by scattering and all light at the forest floor is diffuse (shade), without any sun-flecks. Whereas at higher solar angles, there is a mix of diffuse (shade) and beam (sun-fleck) light. This is consistent with reports of primarily diffuse radiation impinging on the canopy during cloud shadow and direct beam light during clear intervals for the forced cumulus cloud conditions characteristic of the dry season (Kivalov and Fitzjarrald, 2018). The main features of this approach are sketched in Fig. 14.

A two-regime model of light environment could have several applications. First, the change in transmittance with sun angle in the mixed regime might be related to aspects of canopy structure. Next, several features depicted in Fig. 14 might provide a basis for comparisons of understory light environments: a.) the angle-independent value of transmittance (Tr_{dif}) in the diffuse regime, b.) the change in transmittance with change in solar elevation ($\Delta Tr / \Delta el$) in the mixed regime, and the angle (el_{crit}) separating the two regimes. We suspect each of these parameters has testable connections to specific components of canopy structure. The diffuse transmittance, Tr_{dif} , is inversely related to the total amount of occluding material – this can be quantified as stand LAI or surface area density. The critical angle el_{crit} is the angle at which sunflecks first appear and the beam component becomes part of the total light regime. This value will likely depend on canopy vertical and horizontal clumping and may be related to the extinction coefficient. Finally, the increase of transmittance with sun angle, $\Delta Tr / \Delta el$, relates to the angular distribution of lateral opening sizes – these are often presented in reports of hemispherical photography. Finally, such a presentation could be used to estimate the relative contribution of diffuse and beam light and enhance radiation budgets (e.g., Mercado et al., 2007). For example, if the diffuse fraction, Tr_{dif} , is diurnally constant and all transmittance in

excess of this fraction is beam radiation, one may estimate that 25.5% of annual transmission occurs in beam light (varying from 27.8% in the dry season to 24.9% in the wet). Note that the proportion of diffuse

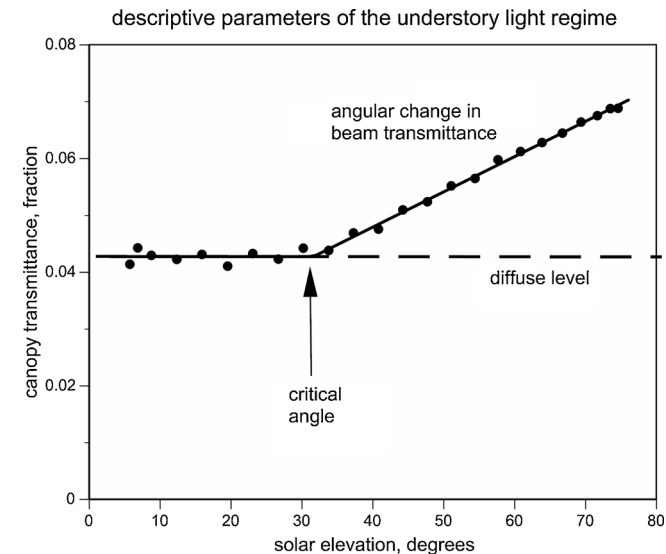


Fig. 14. A representation of canopy transmittance properties for use in comparing diverse reports based on the concept of two light regimes: conditions that are diffuse only and others that are a mixture of diffuse and direct. The parameters illustrated are the diffuse level transmittance, the change in beam transmittance with change in solar angle, and the angle separating these two phases. The values here are the annual mean transmittances shown by season in Fig. 13.

transmittance ($74.5\% = 100 - 25.5\%$) corresponds to a level of $150 \mu\text{mol m}^{-2} \text{s}^{-1}$, about the level at the break in slope of the frequency distribution (inset of Fig. 6) and also near the level at which the duration-frequency relation becomes flat (Fig. 7).

Canopy extinction coefficient. The observations suggest some shortcomings in the extinction coefficient, k, commonly used to describe canopy properties and to estimate transmittance. Variations in the extinction coefficient within a day have been reported in several studies (e.g., Black et al., 1991; Wang et al., 2004). One common model of transmittance-LAI relation (the 'G-function,' Welles and Norman, 1991, LICOR 1992, Welles and Cohen, 1996; Breda, 2003) explicitly accounts for sun and foliage angles. In this study, we also observed daily changes in the coefficient. The variation in the conventional k reflects the daily change in measured transmittance – it assumes a constant effective LAI. Because of these sensitivities to conditions of measurement and aggregation, the extinction coefficient may not be the most suitable descriptor of canopy properties. The alternative approach we suggest may have advantages for comparisons among disparate studies.

4.5. Efficacy of diffuse light transmission

Several studies have suggested that diffuse light is associated with greater conversion of canopy-absorbed PPFD into production (the light

use efficiency, LUE) (e.g., Gu et al., 2002; Yamasoe et al., 2006; Alton et al., 2007; Doughty et al., 2010). Mechanisms proposed for diffuse light efficacy include: 1.) more uniform scattering, 2.) with potential absorption by leaf undersides, 3.) greater LUE of photosynthesis at lower light levels, and, 4.) avoidance of flickering conditions and attendant lags in assimilation. Graham et al. (2003) showed that addition of light during cloudy conditions enhanced tree growth, suggesting some tropical forests might be light limited. However, Kivalov and Fitzjarrald (2019) found enhanced productivity on partly cloudy days can be a result of the alternating light and shadow periods. The averaging of such fluctuating conditions could result in a classification of 'diffuse' skies, possibly obscuring the causal link between sky conditions and LUE.

We found that canopy transmittance was only slightly higher under low brightness conditions - 5.67% for brightness classes I and II compared to 5.59% for classes III and IV (Hutchison et al., 1980) (Table 4). However, as low brightness situations are associated with low PPFD and since these conditions occur only 47.7% of the time, the diffuse effect is negligible to the PAR budget. Note that our estimate of sky brightness (B) does not correspond linearly with the commonly described diffuse fraction. The diffuse fraction tends to be constant at both high and low brightness and between these limits varies rapidly (see Iqbal, 1983; Spitters et al., 1986).

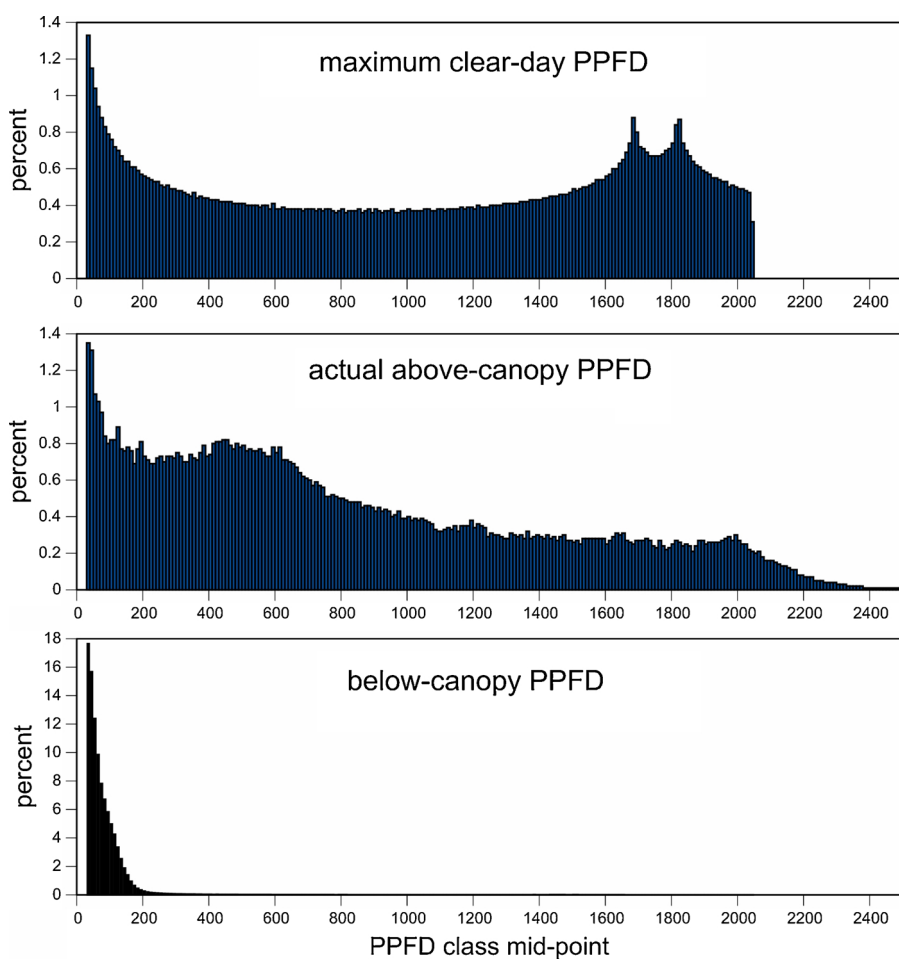


Fig. 15. Frequency distribution of PPFD (scaled to 100%) from the maximum clear day values (top panel), radiation incident at tower top (center panel) and that measured on the forest floor, considering only values > 20 PPFD units. The upper panel values are calculated from the solar elevations at 1 min intervals for an entire year. The center panel derives from the 5-s values at the tower for the days in 2002 and 2003 used to assemble the standard year. The bottom comes from the understory array sensors observed at 10 s intervals.

4.6. Summary and conclusions

A full appreciation of the canopy light environment requires an understanding of sky conditions (rain, clouds and other influences on transmissivity) as well as knowing features of canopy structure. A compelling analogy considers sky and canopy as successive and qualitatively distinct filters, ones that cannot operate independently. This is illustrated by comparing histograms of clear sky, top of canopy incident radiation and forest floor PPFD (Fig. 15). The change between the upper and middle panel is due to the atmosphere filter (clouds mostly but also dust, smoke, aerosols, possibly rain). The change from the middle to the lower panel is due to the canopy and the interaction with solar position.

The top panel has a sharp cut-off around 2100, which follows our model. The pair of peaks, derived from the elevation distributions, is a common feature of elevation distributions at low latitudes. In this angle distribution, the peaks are at $90 - 23.5 \pm 2.85^\circ$, the latitude of km67. Some values in the middle panel are above the maxima of the upper panel - these are likely from transient peaks of enhanced reflected light that precede and follow the towering tropical cumuli (e.g., Gu et al., 2001). The PPFD range from 1400 to 2000 is diminished by cloud presence and enhanced in the 400–600 band compared to the clear-day pattern. The lowest panel is wholly due to canopy presence, which dramatically alters the distribution shape.

The atmosphere is not simply an external forcing – it exists in a two-way interaction with the terrestrial ecosystem. For example, the degree and timing of convective cloudiness – locally forced by transpiration – modulates the available PPFD (Kivalov and Fitzjarrald, 2018, 2019). Seasonal variation in water availability can alter canopy structure and foliage properties, influencing albedo and atmosphere-surface mass exchanges (e.g., Gash and Shuttleworth, 1991; Garratt, 1993). Clouds, often treated as contaminants in remote sensing scenes, have an important influence on the canopy radiation budgets. Occurrence of sunflecks at the forest floor is conditional on there being direct incident sunlight above the canopy, and this depends on sky conditions.

Since radiation in vegetation is variable in many combinations of ways (spatial, temporal and spectral), it is important for understanding the forest radiation environment to observe as many aspects of light as possible. Our attempts to do so were successful in some regards but not in others. Advances in sampling and data processing (e.g., sensor networks) will overcome some of the challenges common to this work. Canopy radiation and structure measurements should be treated as

parts of the continuous data streams we obtain for climate variables. Short-term anecdotal observations, the standard in the past, are clearly insufficient for detailing the long-term and broad-scale light environments. Spatially distributed networks at several levels in the canopy operated over several seasons should be deployed in preference to spot sampling. To allow proper description of the spatial and temporal quality of light in the canopy space, researchers must take care to demonstrate that their observational arrays are commensurate with the characteristic scales of such variability. We note, however, that campaigns to clarify average vertical canopy structure are needed to generalize these statistics to other sites.

Finally, we propose a means to describe noteworthy features of understorey light environments: the background diffuse transmittance, the change in transmittance with solar angle and the angle separating these regimes. This approach: a.) avoids reliance on cumbersome, assumption-fraught models, b.) is straightforward to implement, c.) allows estimates of long-term budgets - including the separation of beam and diffuse components, and, d.) promotes direct comparison among studies.

Acknowledgements

The Large-Scale Biosphere-Atmosphere Experiment in Amazonia (LBA) is an international project, led by Brazil. This project was part of LBA-ECO project group CD-03 and was supported with grants from NASA to the Atmospheric Sciences Research Center (ASRC), University at Albany, SUNY (grants NNG-06GE09A and NCC-5692) with sub-contracts to the Smithsonian Environmental Research Center and, from 2007–2014, by ASRC. Additional support was also provided by the Smithsonian Environmental Research Center. We thank Luiz Medeiros (now at Unipampa, Alegrete RS, Brazil), Júlio Tóta and Rodrigo da Silva (both now at the Universidade Federal do Oeste de Pará, UFOPA), Eleazar Brait, (then at the LBA Project Office, Santarém), Alexander Tsosyref and Matt Czikowsky (ASRC), and Ralf Staebler (ASRC, now at Environment Canada) and Ricardo Sakai (ASRC, now at Howard University) for help in the field; Rodrigo da Silva (UFOPA) provided the site location figure; and Dieter Anhuf (Universität Passau) and Rüter Rollenbeck (Philipps Universität Marburg) for PPFD profile data from the Surumoni forest. Support to complete this analysis and publish the manuscript was provided through grant ER65583/SC0011120 from the US Department of Energy to ASRC, as part of the GO-Amazon Project.

Appendix A. Canopy reflectance measures

See Fig. A1

We observed a seasonal difference in the ratio of canopy reflectances between the visible (PAR_{ref}) and near infrared (NIR_{ref}) wavebands using our combination index (cbNDVI). The values of the index are among the higher observed for closed forests (e.g., Huemmrich et al., 1999) and show a difference between seasons. Similar observations from remote sensing have been reported for the study area (using MODIS: Huete et al., 2002 and Doughty and Goulden, 2008; using SPOT: Xiao et al., 2005). The higher values of index in the wet season have been interpreted to indicate greater leaf area (Myndeni et al., 1995; Sellers, 1985). However, we found no evidence of significant seasonal changes in LAI (Table 1), although we did observe some reduction in transmittance in the wet season compared with the dry (Table 4). Malhado et al. (2009) also found only slight seasonal LAI variation at this site in 2004.

Several authors have reported that the central Amazonian forest exhibits a seasonal greenness change (da Rocha et al., 2004; Huete et al., 2006; Myndeni et al., 2007; Saleska et al., 2007; Doughty and Goulden, 2008; Brando et al., 2010) and Net Ecosystem Exchange (Saleska et al., 2003) that might be exacerbated by droughts (Phillips et al., 2009). Much attention has been given to this possibility for the year 2005 (e.g. Samanta et al., 2010 and 2012). Since our study concluded in 2004 we can offer no evidence directly relevant to this debate. However, we note that this discussion is more than just about drought effects. In the non-drought conditions of 2002–2004 we observed seasonal changes in the forest reflective properties (Fig. 13; Table 3), but it was accompanied by little change in the canopy structure related to transmittance.

Our results do provide some ancillary information of use in the seasonal change debate. Morton et al. (2014) constructed the Bidirectional Reflectance Distribution Function (BRDF) to examine NDVI for scenes that played a role in this discussion. We note that our measurements allow us to examine the approximate NDVI estimate, the cbNDVI for a wide variety of sun angles, though we lack view angle variation since our sensors have a broad field-of-view. These data complement information from the space-borne observations made from a limited number of sun-angle and view angle cases used to compose the BRDF.

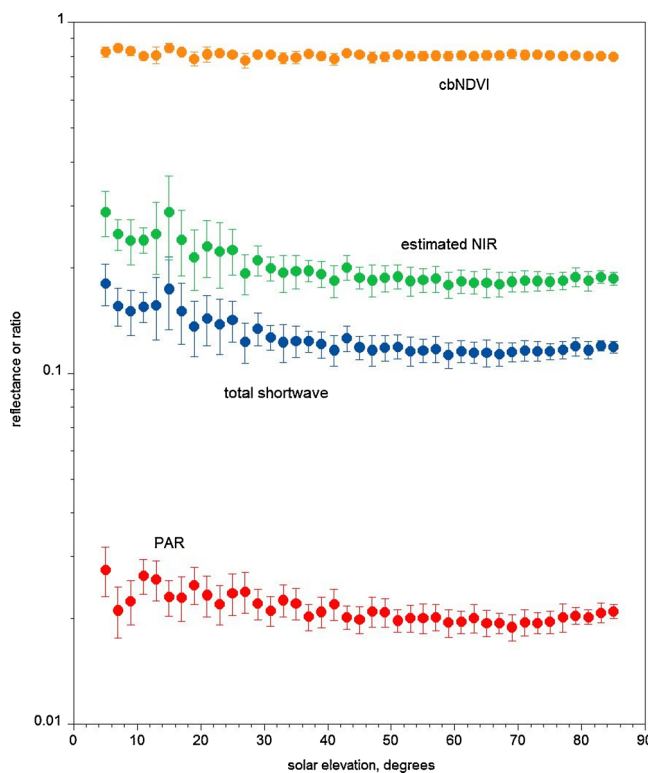


Fig. A1. Solar elevation dependence of canopy reflectance of PPFD, shortwave radiation, estimated NIR and the composite broadband reflectance index, cbNDVI, for brightness classes I and II and solar elevations above 5°. Plotted values are means and standard deviations for 2° wide angle classes.

References

- Alton, P.B., North, P.R., Los, S.O., 2007. Effect of diffuse sunlight on canopy-use efficiency, gross photosynthetic product and net ecosystem exchange in three forest biomes. *Global Change Biol.* 13, 776–787.
- Anhuf, D., Rollenbeck, R., 2001. Canopy structure of the Rio surumoni rain forest (Venezuela) and its influence on microclimate. *Ecotropica* 7, 21–32.
- Ashton, P.S., 1958. Light intensity measurements in rain forest near Santarem, Brazil. *J. Ecol.* 46, 65–70.
- Asner, G.P., 2001. Cloud cover in Landsat observations of the Brazilian Amazon. *Int. J. Remote Sens.* 22 (18), 3855–3862.
- Asner, G.P., Keller, M., Pereira Jr, R., Zweede, J.C., Silva, J.N.M., 2004. Canopy damage and recovery after selective logging in Amazonia: field and satellite studies. *Ecol. Appl.* 14, S280–S298.
- Baldocchi, D.D., Collineau, S., 1994. The physical nature of solar radiation in heterogeneous canopies, spatial and temporal attributes. Pp. 21–21471. In: Caldwell, M.M., Pearcy, R.W. (Eds.), *Exploitation of Environmental Heterogeneity by Plants – Ecophysiological Processes Above-and Belowground*. Academic Press, Inc, pp. 429.
- Barradas, V.L., 1991. Radiation regime in a tropical dry deciduous forest in western Mexico. *Theor. Appl. Climatol.* 44, 57–64.
- Barradas, V.L., Adem, J., 1992. Albedo model for a tropical dry deciduous forest in western Mexico. *Int. J. Biometeorol.* 36, 113–117.
- Becker, P., Smith, A., 1990. Spatial autocorrelation of solar radiation in a tropical moist forest understory. *Agri. Forest Meteorol.* 52, 373–379.
- Bjorkman, O., Ludlow, M.M., 1972. Characterization of the light climate on the forest floor of a Queensland rainforest. *Carnegie Inst. Washington Yearbook* 71, 85–94.
- Black, T.A., Chen, J.-M., Lee, X., Sagar, R.M., 1991. Characteristics of shortwave and longwave irradiances under a Douglas-fir forest stand. *Can. J. For. Res.* 21, 1020–1028.
- Brando, P., Goetz, S., Baccini, A., Nepstad, D., Beck, P., Christman, M., 2010. Seasonal and interannual variability of climate and vegetation indices across the Amazon. *Proc. National Academy Sci. USA* 107, 14685.
- Breda, N.J.J., 2003. Ground-based measurements of leaf area index: a review of methods, instruments and current controversies. *J. Exp. Bot.* 54, 2403–2417.
- Brinkmann, W.L.F., 1971. Light environment in a tropical rainforest of central Amazonia. *Acta Amazonica* 1, 37–49.
- Brown, M.J., Parker, G.G., Posner, N., 1994. A survey of ultraviolet-B radiation in forests. *J. Ecology* 82, 843–853.
- Čermák, J., 1989. Solar equivalent leaf area: an efficient biometrical parameter of individual leaves, trees and stands. *Tree Physiol.* 5, 269–289.
- Chambers, J.Q., dos Santos, J., Ribeiro, R.J., Higuchi, N., 2001. Tree damage, allometric relationships, and aboveground net primary production in a central rainforest. *For. Ecol. Manage.* 152, 73–84.
- Chazdon, R.L., 1988. Sunflecks and their importance to forest understory plants. *Adv. Ecolo. Res.* 18, 1–63.
- Chazdon, R.L., Fetterer, N., 1984. Photosynthetic light environments in a lowland tropical rainforest in Costa Rica. *J. Ecol.* 72, 553–564.
- Chen, J.M., 1996. Optically based methods for measuring seasonal variation in leaf area index of boreal conifer forests. *Agric. For. Meteorol.* 80, 135–163.
- Clark, D.B., Clark, D.A., Rich, P.M., Weiss, S., Oberbauer, S.F., 1996. Landscape-scale evaluation of understory light and canopy structure: methods and application in a neotropical lowland rain forest. *Can. J. For. Res.* 26, 747–757.
- Cohen, J.C.P., Fitzjarrald, D.R., D’Oliveira, F.A.F., Saraiva, I., Barbosa, I.R.D.S., Gandu, A.W., Kuhn, P.A., 2014. Radar-observed spatial and temporal rainfall variability near the Tapajós-Amazon confluence. *Revista Brasileira de Meteorologia* 29 (SPE, 23–30).
- Cournac, L., Dubois, M.A., Chave, J., Riera, B., 2002. Fast determination of light availability and leaf area index in tropical forests. *J. Trop. Ecology* 18, 295–302.
- Czikowsky, M.J., Fitzjarrald, D.R., 2009. Detecting rainfall interception in an Amazonian rain forest with eddy flux measurements. *J. Hydrol.* 377, 92–105.
- Da Rocha, H.R., Goulden, M.L., Miller, S.D., Menton, M.C., Pinto, L.D.V.O., deFreita, H.C., SolvaFigueira, A.M., 2004. Seasonality of water and heat fluxes over a tropical forest in Eastern Amazonia. *Ecol. Appl.* 14 (Suppl.), S22–S32.
- Davidson, E.A., Artaxo, P., 2004. Globally significant changes in biological processes of the Amazon Basin: results of the large-scale Biosphere-Atmosphere Experiment. *Global Change Biol.* 10, 519–529.
- De Castilho, C., Magnusson, W., de Araújo, R., Luizão, R., Lima, A., et al., 2006. Variation in aboveground tree live biomass in a central Amazonian forest: effects of soil and topography. *For. Ecol. Manage.* 234, 85–96.
- De Wasseige, C., Bastin, D., DeFourny, P., 2003. Seasonal variation of tropical forest LAI based on field measurements in Central African Republic. *Agric. For. Meteorol.* 119, 181–194.
- Domingues, T., Berry, J., Martinelli, L., Ometto, J., Ehleringer, J., 2005. Parameterization of canopy structure and leaf-level gas exchange for an eastern Amazonian tropical rain forest (Tapajós National Forest, Pará, Brazil). *Earth Interact.* 9, 1–23.
- Doughty, C.E., Goulden, M.L., 2008. Seasonal patterns of tropical forest leaf area index and CO₂ exchange. *J. Geophys. Res.* 113, G00B06. <https://doi.org/10.1029/2007JG000590>.
- Doughty, C.E., Flanner, M.G., Goulden, M.L., 2010. Effect of smoke on subcanopy shaded light, canopy temperature, and carbon dioxide uptake in an Amazon rainforest. *Global Biogeochem. Cycles* 24, GB3013. <https://doi.org/10.1029/2009GB003670>.
- Emmons, L.H., Chatelet, P., Cournac, L., Pitman, N.C.A., del Aguilera, L.F., Dubois, M.A., 2006. Seasonal change in leaf area index at three sites along a South American latitudinal gradient. *Ecotropica* 12, 87–102.
- Espírito-Santo, F.D., Keller, M.M., Linder, E., Oliveira Junior, R.C., Pereira, C., Oliveira, C.G., 2014. Gap formation and carbon cycling in the Brazilian Amazon: measurement using high-resolution optical remote sensing and studies in large forest plots. *Plant Ecol. Divers* 7, 305–318.

- Fitzjarrald, D.R., Sakai, R.K., Moraes, O.L.L., de Oliveira, R.C., Acevedo, O.C., Czikowsky, M.J., Beldini, T., 2008. Spatial and temporal rainfall variability near the amazon-tapajós confluence. *J. Geophys. Res.* 113. <https://doi.org/10.1029/2007JG000596>.
- Freedman, J.M., Fitzjarrald, D.R., Moore, K.E., 2001. Boundary layer clouds and vegetation-atmosphere feedbacks. *J. Clim.* 14, 180–197.
- Garratt, J.R., 1993. Sensitivity of climate simulations to land surface and atmospheric boundary layer treatments: a review. *J. Climatol.* 6, 419–449.
- Gash, J.H.C., Shuttleworth, W.J., 1991. Tropical deforestation: albedo and the surface-energy balance. *Clim. Change* 19, 123–133.
- Goulden, M.L., Miller, S.D., da Rocha, H.R., Menton, M.C., de Freitas, H.C., Figueira, A.E.S., de Sousa, C.A.D., 2004. Diel and seasonal patterns of tropical forest CO₂ exchange. *Ecol. Appl.* 14 (Supplement), S24–S54.
- Gower, S.T., Kucharik, C.J., Norman, J.M., 1999. Direct and indirect estimation of leaf area index, fAPAR, and net primary production of terrestrial ecosystems. *Remote Sens Environ.* 70 (1), 29–51.
- Graham, E.A., Mulkey, S.S., Wright, S.J., Kitajima, K., Phillips, N.G., 2003. Cloud cover limits CO₂ uptake and growth of a rainforest tree during tropical rainy seasons. *Proc. National Acad. Sci.* 100, 572–576.
- Grubb, P.J., Whitmore, T.C., 1967. A comparison of montane and lowland forest in Ecuador. III. The light reaching the ground vegetation. *J. Ecol.* 47, 33–57.
- Gu, L., Fuentes, J.D., Garstang, M., da Silva, J.T., Heitz, R., Sigler, J., Shugart, H.H., 2001. Cloud modulation of surface solar irradiance at a pasture site in southern Brazil. *Agric. For. Meteorol.* 106 (2), 117–129.
- Gu, L., Baldocchi, D., Verma, S.B., Black, T.A., Vesala, T., Falge, E.M., Dowty, P.R., 2002. Advantages of diffuse radiation for terrestrial ecosystem productivity. *J. Geophys. Res.* 107 (D6), 4050. <https://doi.org/10.1029/2001JD001242>.
- Hassika, P., Berbigier, P., 1998. Annual cycle of photosynthetically active radiation in a maritime pine forest. *Agric. For. Meteorol.* 90, 151–171.
- Huemmrich, K.F., Black, T.A., Jarvis, P.G., McCaughey, J.H., Hall, F.G., 1999. High temporal resolution NDVI phenology from micrometeorological radiation sensors. *J. Geophys. Res.* 11 (D22), 27935–27944.
- Huete, A.R., Didan, K., Miura, T., Rodriguez, E.P., Gao, X., Ferreira, L.G., 2002. Overview of the radiometric and biophysical performance of the MODIS vegetation indices. *Remote Sens. Environ.* 83, 195–213.
- Huete, A.R., Didan, K., Shimabukuro, Y.E., Ratana, P., Saleska, S.R., Hutyra, L.R., Yang, W.Z., Nemani, R.R., Myneni, R., 2006. Amazon rainforests green-up with sunlight in dry season. *Geophys. Res. Lett.* 33, L06405.
- Hutchison, B.A., Matt, D.R., McMillen, R.T., 1980. Effects of sky brightness distribution upon transmission of diffuse radiation through canopy gaps in a deciduous forest. *Agri. Meteorol.* 22, 137–147.
- Hutyra, L.R., Munger, J.W., Nobre, C.A., Saleska, S.R., Vieira, S.A., Wofsy, S.C., 2005. Climatic variability and vegetation vulnerability in amazonia. *Geophys. Res. Lett.* 32, L24712. <https://doi.org/10.1029/2005GL024981>.
- Iqbal, M., 1983. An Introduction to Solar Radiation. Academic Press, New York.
- Januário, M., Viswanadham, Y., Senna, R.C., 1992. Radiação solar total dentro e fora de floresta tropical úmida de terra firme (tucurí, pará). *Acta Amazonica* 22, 335–340.
- Jones, H.G., Archer, N., Rotenberg, E., Casa, R., 2003. Radiation measurement for plant physiology. *J. Exp. Bot.* 54, 879–889.
- Keller, M., Palace, M., Hurt, G., 2001. Biomass estimation in the tapajos national Forest, Brazil: examination of sampling and allometric uncertainties. *For. Ecol. Manage.* 154, 371–382.
- Keller, M., Alencar, A., Asner, G.P., Braswell, B., Bustamante, M., Davidson, E., Feldpausch, T., Fernandes, E., Goulden, M., Kabat, P., Kruitj, B., Luizão, F., Miller, S., Markewitz, D., Nobre, A.D., Nobre, C.A., Priante Filho, N., da Rocha, H., Silva Dias, P., von Randow, C., Vourlitis, G.L., 2004. Ecological research in the large-scale biosphere-atmosphere experiment in amazonia: early results. *Ecol. Appl.* 14, S3–S16.
- Kivalov, S.N., Fitzjarrald, D.R., 2018. Quantifying and modelling the effect of cloud shadows on the surface irradiance at tropical and midlatitude forests. *Boundary Layer Meteorol.* 166 (2), 1–34.
- Kivalov, S.N., Fitzjarrald, D.R., 2019. Observing the whole-canopy short-term dynamic response to natural step changes in incident light: characteristics of tropical and temperate forests. *Boundary-Layer Meteorol.* [https://doi.org/10.1007/s10546-019-00000-0](https://doi.org/10.10.1007/s10546-019-00000-0).
- Koizumi, H., Oshima, Y., 1993. Light environment and carbon gain of understory herbs associated with sunflecks in a warm temperate deciduous forest in Japan. *Ecol. Res.* 8, 135–142.
- Kotchenova, S.Y., Song, X.D., Shabanova, N.V., Potter, C.S., Knyazikhin, Y., Myneni, R.B., 2004. Lidar remote sensing for modeling gross primary production of deciduous forests. *Remote Sens. Environ.* 92, 158–172.
- Küppers, M., Timm, H., Orth, F., Stegemann, J., Stöber, R., Scheider, H., Paliwal, K., Karunaichamy, K.S.T.K., Ortiz, R., 1996. Effect of light environment and successional status on lightfleck use by understory trees of temperate and tropical forests. *Tree Physiol.* 16, 69–80.
- Lang, A.R.G., 1986. Leaf area and average leaf angle from transmission of direct sunlight. *Aust. J. Bot.* 34, 349–355.
- Lang, A.R.G., 1987. Simplified estimate of leaf area index from transmittance of the sun's beam. *Agri. Forest Meteorol.* 41, 179–186.
- Lee, D.W., 1989. Canopy dynamics and light climates in a tropical moist deciduous forest in India. *J. Trop. Ecol.* 5 (1), 65–79.
- Lee, H., Slatton, K.C., Roth, B.E., Cropper, W.P., 2009. Prediction of forest canopy light interception using three dimensional airborne LiDAR data. *Int. J. Remote Sens.* 30, 189–207.
- Leitão, M.M.V.B.R., Santos, J.M., Oliveira, G.M., 2002. Estimativas do albedo em treés ecossistemas de floresta amazônica. *Rev. Bras. Eng. Agric. Ambient.* 6, 256–261.
- Leitold, V., 2009. Canopy Structure and Function in the Tapajós National Forest in Equatorial Amazonia, Brazil. B.S. Thesis. Harvard College, Cambridge MA.
- Li, R., Min, Q., 2013. Dynamic response of microwave land surface properties to precipitation in amazon rainforest. *Remote Sens. Environ.* 133, 183–192.
- LI-COR, 1992. LAI-2000 Plant Canopy Analyzer Operating Manual. LI-COR, Inc., Lincoln NE.
- LI-COR, 2005. LI-COR Terrestrial Radiation Sensors Instruction Manual. LI-COR, Inc., Lincoln NE.
- Mahli, Y., Aragão, L., Metcalfe, D., Paiva, R., Quesada, C., Almeida, S., et al., 2009. Comprehensive assessment of carbon productivity, allocation and storage in three amazonian forests. *Global Change Biol.* 15, 1255–1274.
- Malhado, A.C.M., Costa, M.H., de Lima, F.Z., Portilho, K.C., Figueiredo, D.N., 2009. Seasonal leaf area dynamics in an amazonian tropical forest. *For. Ecol. Manage.* 258, 1161–1165.
- Marques Filho, A.O., Dallarosa, R.G., 2000. Interceptação de radiação solar e distribuição espacial de área foliar em floresta de terra firme da amazônia Central. *Acta Amazonica* 30, 453–470.
- Marques Filho, A.O., Dallarosa, R.G., 2001. Atenuação de radiação solar e distribuição vertical de área foliar em floresta reserva jaru, rondonia, Brasil. *Acta Amazonica* 31, 39–59.
- Marques Filho, A.O., Dallarosa, R.G., Pachêco, V.B., 2005. Radiação solar e distribuição vertical de área foliar em floresta reserva biológica do cuiabá ZF2, Manaus. *Acta Amazonica* 35, 427–436.
- McWilliam, A., Roberts, J., Cabral, O., Leitao, M., De Costa, A., Maitelli, G., Zamparoni, C.A.G., 1993. Leaf area index and above-ground biomass of terra firme rain forest and adjacent clearings in amazonia. *Funct. Ecol.* 7, 310–317.
- Mercado, L.M., Huntingford, C., Gash, J., Cox, P.M., Jigmeddy, V., 2007. Improving the representation of radiation interception and photosynthesis for climate model applications. *Tellus* 59B, 553–565.
- Miller, J.B., 1967. A formula for average foliage density. *Aus. J. Botany* 15, 141–144.
- Miller, S.D., Goulden, M.L., Menton, M.C., Da Rocha, H.R., de Freitas, H.C., Silva Figueira, A.M., De Sousa, C.A.D., 2004. Biometric and micrometeorological measurements of tropical forest carbon balance. *Ecol. Appl.* 14 (Supplement 4), S114–S126.
- Mizoguchi, Y., Ohtani, Y., Aoshima, T., Hirakata, A., Yuta, S., Takanashi, S., Iwata, H., Nakai, Y., 2010. Comparison of the characteristics of five quantum sensors. *Bulletin FFPRI* 9, 113–120.
- Monsi, M., Saeki, T., 1953. Über den lichtfaktor in den pflanzengesellschaften und seine bedeutung für die stoffproduktion. *Jap. J. Bot.* 14, 22–52.
- Montgomery, R.A., Chazdon, R.L., 2001. Forest structure, canopy architecture, and light transmittance in tropical wet forests. *Ecology* 82, 2707–2718.
- Moore, K.E., Fitzjarrald, D.R., Sakai, R.K., Goulden, M.L., Munger, J.W., Wofsy, S.C., 1996. Seasonal variation in radiative and turbulent exchange at a deciduous forest in central Massachusetts. *J. Appl. Meteorol.* 35 (122), 134.
- Morton, D.C., Nagol, J., Carabajal, C.C., Rosette, J., Palace, M., Cook, B.D., Vermote, E.F., Harding, D.J., North, P.R.J., 2014. Amazon forests maintain consistent canopy structure and greenness during the dry season. *Nature* 506, 221–224. <https://doi.org/10.1038/nature13006>.
- Myneni, R.B., Hall, F.G., Sellers, P.J., Marshak, A.L., 1995. The interpretation of spectral vegetation indexes. *IEEE Trans. Geosciences Remote Sensing* 33, 481–486.
- Myneni, R.B., Yang, W., Nemani, R.R., Huete, A.R., Dickinson, R.E., et al., 2007. Large seasonal swings in leaf area of amazon rainforests. *Proc. National Acad. Sci. USA* 104, 4820–4823.
- Naumburg, E., Ellsworth, D.S., 2000. Photosynthetic sunfleck utilization potential of understory saplings growing under elevated CO₂ in FACE. *Oecologia* 122, 163–174.
- Nicotra, A.B., Chazdon, R.L., Iriarte, S.V.B., 1999. Spatial heterogeneity of light and woody seedling regeneration in tropical wet forests. *Ecology* 80, 1908–1926.
- Palace, M., Keller, M., Asner, G.P., Hagen, S., Braswell, B., 2008. Amazon forest structure from IKONOS satellite data and the automated characterization of forest canopy properties. *Biotropica* 40, 141–150.
- Parker, G.G., Russ, M.E., 2004. The canopy surface and stand development: assessing forest canopy structure and complexity with near-surface altimetry. *For. Ecol. Manage.* 189, 307–315.
- Parker, G.G., Lefsky, M.A., Harding, D.J., 2001. PAR transmittance in forest canopies determined from airborne LiDAR altimetry and from in-canopy quantum measurements. *Remote Sens. Environ.* 76, 298–309.
- Parker, G.G., Chapoton, S.M., Davis, M., 2002. Canopy light transmittance in an age sequence of Douglas-fir/western hemlock stands. *Tree Physiol.* 22, 147–157.
- Parker, G.G., Harding, D.J., Berger, M., 2004a. A portable LiDAR system for rapid determination of forest canopy structure. *J. Appl. Ecol.* 41, 755–767.
- Parker, G.G., Harmon, M.E., Lefsky, M.A., Chen, J., Van Pelt, R., Weiss, S.B., Thomas, S.C., Winner, W.E., Shaw, D.C., Franklin, J.F., 2004b. Three-dimensional structure of an old-growth *Pseudotsuga-Tsuga* canopy and its implications for radiation balance, microclimate, and atmospheric gas exchange. *Ecosystems* 7, 440–453.
- Parker, G.G., Tinoco-Ojaguren, C., Martínez-Yrízar, A., Maass, M., 2005. Seasonal balance and vertical pattern of photosynthetically active radiation within canopies of a tropical dry deciduous forest ecosystem in México. *J. Trop. Ecology* 21, 283–295.
- Parrotta, J.A., Francis, J.K., de Almeida, R.R., 1995. Trees of the Tapajós: a Photographic Field Guide. USDA Forest Service, General Technical Report IITF-1, Rio Piedras PR.
- Pearcy, R.W., 1990. Sunflecks and photosynthesis in plant canopies. *Ann. Rev. Plant Physiol. Plant Mol.* Biology 41, 4241–4453.
- Phillips, O.L., Aragão, L.E.O.C., Lewis, S.L., Fisher, J.B., Lloyd, J., López-González, G., Malhi, Y., Monteagudo, A., Peacock, J., et al., 2009. Drought sensitivity of the amazon rainforest. *Science* 323, 1344–1347.
- Pike, R.J., Wilson, S.E., 1971. Elevation relief ratio, hypsometric integral and geomorphic area-altitude analysis. *Geol. Soc. Am. Bull.* 82, 1079–1084.
- Price, D.T., Black, T.A., 1990. Effects of short-term variation in weather on diurnal canopy CO₂ flux and evapotranspiration of a juvenile Douglas-fir stand. *Agric. For. Meteorol.* 50, 139–158.
- Pyle, E.H., Santoni, G.W., Nascimento, H.E.M., Hutyra, L.R., Vieira, S., Curran, D.J., van

- Haren, J., Saleska, S.R., Chow, V.Y., Carmago, P.B., Laurance, W.F., Wofsy, S.C., 2008. Dynamics of carbon, biomass, and structure in two amazonian forests. *J. Geophys. Res. – Biogeosciences* 113, G00B08.
- Rice, A., Pyle, E., Saleska, S., Hutyra, L., Palace, M., Keller, M., de Camargo, P., Portillo, K., Marques, D., Wofsy, S., 2004. Carbon balance and vegetation dynamics in an old-growth amazonian forest. *Ecol. Appl.* 14, S55–S71.
- Rivard, J.C., Quesada, M., 2005. Effects of season and successional stage on leaf area index and spectral vegetation indices in three mesoamerican tropical dry forests. *Biotropica* 37, 486–496.
- Ross, J., Möttus, M., 2000. Statistical treatment of sunfleck length inside willow coppice. *Agric. For. Meteorol.* 104, 215–231.
- Sakai, R.K., Fitzjarrald, D.R., Moraes, O.L., Staebler, R.M., Acevedo, O.C., Czikowsky, M.J., Silva, R.D., Brait, E., Miranda, V., 2004. Land-use change effects on local energy, water, and carbon balances in an amazonian agricultural field. *Global Change Biol.* 10 (5), 895–907.
- Saleska, S.R., Miller, S.D., Matross, D.M., et al., 2003. Carbon in amazon forests: unexpected seasonal fluxes and disturbance-induced losses. *Science* 302, 1554–1557.
- Saleska, S.R., Didan, K., Huete, A.R., da Rocha, H.R., 2007. Amazon forests green-up during 2005 drought. *Science* 318, 612.
- Samanta, A., Ganguly, S., Hashimoto, H., Devadiga, S., Vermote, E., Knyazikhin, Y., Nemani, R.R., Myneni, R.B., 2010. Amazon forests did not green-up during the 2005 drought. *Geophys. Res. Lett.* 37, L05401. <https://doi.org/10.1029/2009GL042154>.
- Samanta, A., Ganguly, S., Vermote, E., Nemani, R.R., Myneni, R.B., 2012. Interpretation of variations in MODIS-measured greenness levels of amazon forests during 2000 to 2009. *Environ. Res. Lett.* 7, 024018. <https://doi.org/10.1088/1748-9326/7/2/024018>.
- SAS Institute, Inc, 2008. SAS Procedures Guide, Version 9.2. SAS Institute Inc., Cary, NC, USA.
- Sellers, P.J., 1985. Canopy reflectance, photosynthesis and transpiration. *Int. J. Remote Sens.* 6, 1335–1372.
- Senna, M.C.A., Costa, M.H., Shimabukuro, Y.E., 2005. Fraction of photosynthetically active radiation absorbed by amazon tropical forest: a comparison of field measurements, modeling, and remote sensing. *J. Geophys. Res.* 110, G01008.
- Smith, A.P., Hogan, K.P., Idol, J.R., 1992. Spatial and temporal patterns of light and canopy structure in a lowland tropical moist forest. *Biotropica* 24, 503–511.
- Sokal, R.R., Rohlf, F.J., 1995. Biometry, third ed. W.H. Freeman Co., New York.
- Spitters, C.J.T., Toussaint, H.A.J.M., Goudriaan, J., 1986. Separating the diffuse and direct component of global radiation and its implications for modeling canopy photosynthesis. Part I. Components of incoming radiation. *Agric. For. Meteorol.* 38, 217–229.
- Stark, S.C., Leitold, V., Wu, J.L., Hunter, M.O., de Castilho, C.V., Costa, F.R.C., McMahon, S.M., Parker, G.G., Shimabukuro, M., Lefsky, M.A., Keller, M., Alves, L.F., Schietti, J., Shimabukuro, Y.E., Brandão, D.O., Woodcock, T.K., Higuchi, N., de Camargo, P.B., de Oliveira, R.C., Saleska, S.R., 2012. Amazon forest carbon dynamics predicted by profiles of canopy leaf area and light environment. *Ecology Letters.* <https://doi.org/10.1111/j.1461-0248.2012.01864.x>.
- Sugita, M., Kotoda, K., 1991. Seasonal variation of albedo of a pine forest. *Hydro. J. Japanese Assoc. Hydrolo. Sci.* 21, 103–108.
- Tang, H., Dubayah, R., Swatantran, A., Hofton, M., Sheldon, S., Clark, D.B., Blair, B., 2012. Retrieval of vertical LAI profiles over tropical rain forests using waveform lidar at La selva, Costa Rica. *Remote Sens. Environ.* 124, 242–250.
- Tarboton, D.G., Bras, R.L., Rodriguez-Iturbe, I., 1989. Scaling and elevation in river networks. *Water Resour. Res.* 25, 2037–2051.
- Thimijian, R.W., Heins, R.D., 1983. Photometric, radiometric, and quantum light units of measure: a review of procedures for interconversion. *HortScience* 19, 818–892.
- Thomas, V., Finch, D.A., McCaughey, J.H., Noland, T., Rich, L., Treitz, P., 2006. Spatial modelling of the fraction of photosynthetically active radiation absorbed by a boreal mixedwood forest using a lidar-hyperspectral approach. *Agric. For. Meteorol.* 140, 287–307.
- Todd, W.T., Scillag, F., Atkinson, P.M., 2003. Three-dimensional mapping of light transmittance and foliage distribution using lidar. *Canadian J. Remote Sensing* 29, 544–555.
- Torquebiau, E.F., 1988. Photosynthetically active radiation environment, patch dynamics and architecture in a tropical rainforest in sumatra. *Aus. J. Plant Physiology* 15, 327–342.
- Tóta, J., Fitzjarrald, D.R., Staebler, R.M., Sakai, R.K., Moraes, O.M.M., Acevedo, O.C., Wofsy, S.C., Manzi, A.O., 2008. Amazon rain forest subcanopy flow and the carbon budget: santarém LBA-ECO site. *J. Geophys. Res. – Biogeosciences* 113, G00B02. <https://doi.org/10.1029/2007JG000597>.
- Trichon, V., Walter, J.-M.N., Laumonier, Y., 1998. Identifying spatial patterns in the tropical rain forest structure using hemispherical photographs. *Plant Ecology* 137, 227–244.
- Viera, S., De Camargo, P., Selhorst, D., Da Silva, R., Hutyra, L., Chambers, J., Brown, I., Higuchi, N., Dos Santos, J., Wofsy, S., et al., 2004. Forest structure and carbon dynamics in amazonian tropical rain forests. *Oecologia* 140, 468–479.
- Vierling, L.A., Wessman, C.A., 2000. Photosynthetically active radiation heterogeneity within a monodominant Congolese rain forest canopy. *Agric. For. Meteorol.* 103, 265–278.
- Vourlitis, G.L., Filho, N.P., Hayashi, M.M.S., Nogueira, J.D.S., Raiter, F., Hoegel, W., Campelo Jr., J.H., 2004. Effects of meteorological variations on the CO₂ exchange of a Brazilian transitional tropical forest. *Ecol. Appl.* 14 (Supplement), S89–S100.
- Walraven, R., 1978. Calculating the position of the sun. *Sol. Energy* 20, 393–397.
- Walraven, R., 1979. Erratum. *Sol. Energy* 22, 195.
- Walter, J.-M.N., Grégoire Himmeler, C., 1996. Spatial heterogeneity of a scots pine canopy: an assessment by hemispherical photographs. *Can. J. For. Res.* 26, 1610–1619.
- Wandelli, E.V., Marques Filho, Ade O., 1999. Medidas de radiação solar e índice de área foliar em coberturas vegetais. *Acta Amazonica* 29, 57–58.
- Wang, Q., Tenhunen, J., Granier, A., Reichstein, M., Bouriaud, O., Nguyen, D., Breda, N., 2004. Long-term variations in leaf area index and light extinction in a *Fagus sylvatica* stand as estimated from global radiation profiles. *Theor. Appl. Climatol.* 79, 225–238.
- Welles, J.M., Cohen, S., 1996. Canopy structure measurement by gap fraction analysis using commercial instrumentation. *J. Exp. Bot.* 47, 1335–1342.
- Welles, J.M., Norman, J.M., 1991. Instrument for indirect measurement of canopy architecture. *Agron. J.* 83, 818–825.
- Wilkinson, B.J., 1981. An improved FORTRAN program for the rapid calculation of the solar position. *Sol. Energy* 27, 67–68.
- Williams, M., Malhi, Y., Nobre, A., Rastetter, E., Grace, J., Pereira, M., 1998. Seasonal variation in net carbon exchange and evapotranspiration in a Brazilian rain forest: a modeling analysis. *Plant, Cell Environ.* 21, 953–968.
- Wirth, R., Weber, B., Ryell, R.J., 2001. Spatial and temporal variability of canopy structure in a tropical moist forest. *Acta Oecologica* 22, 235–244.
- Xiao, X., Zhang, Q., Saleska, S., Huytra, L., de Camargo, P., Wofsy, S., Frolking, S., Boles, S., Keller, M., Moore III, B., 2005. Satellite-based modeling of gross primary production in a seasonally moist tropical rainforest. *Remote Sens. Environ.* 94, 105–122.
- Yamasoe, M.A., von Randow, C., Manzi, A.O., Schafer, J.S., Eck, T.F., Holben, B.N., 2006. Effect of smoke and clouds on the transmissivity of photosynthetically active radiation inside the canopy. *Atmos. Chem. Phys.* 6, 1645–1656.
- Yoda, K., 1978. The three-dimensional distribution of light intensity in a tropical rain forest in West Malaysia. *Japanese J Ecol.* 24, 247–254.
- Yoshimura, M., Yamashita, M., 2012. Measurement of tropical rainforest three-dimensional light environment and its diurnal change. *Int. J. Remote Sens.* 33, 848–859.
- Young, D.R., Smith, W.K., 1979. Influence of sunflecks on the temperature and water relations of two understory congeners. *Oecologia* 43, 192–205.